

# UC Irvine

## UC Irvine Previously Published Works

### Title

Autoimmune Manifestations in the 3xTg-AD Model of Alzheimer's Disease

### Permalink

<https://escholarship.org/uc/item/9bp0208d>

### Journal

Journal of Alzheimer's Disease, 39(1)

### ISSN

1387-2877

### Authors

Marchese, Monica  
Cowan, David  
Head, Elizabeth  
[et al.](#)

### Publication Date

2014

### DOI

10.3233/jad-131490

Peer reviewed



Published in final edited form as:

*J Alzheimers Dis.* 2014 ; 39(1): 191–210. doi:10.3233/JAD-131490.

## Autoimmune Manifestations in the 3xTg-AD Model of Alzheimer's Disease

Monica Marchese<sup>a</sup>, David Cowan<sup>b</sup>, Elizabeth Head<sup>f</sup>, Donglai Ma<sup>c</sup>, Khalil Karimi<sup>b</sup>, Vanessa Ashthorpe<sup>e</sup>, Minesh Kapadia<sup>d</sup>, Hui Zhao<sup>d</sup>, Paulina Davis<sup>f</sup>, and Boris Sakic<sup>d,\*</sup>

<sup>a</sup> Department of Clinical Epidemiology and Biostatistics, McMaster University, Hamilton, ON, Canada

<sup>b</sup> Department of Medicine, McMaster University, Hamilton, ON, Canada

<sup>c</sup> Department of Pathology and Molecular Medicine, McMaster University, Hamilton, ON, Canada

<sup>d</sup> Department of Psychiatry & Behavioral Neurosciences, McMaster University, Hamilton, ON, Canada

<sup>e</sup> Central Animal Facility, McMaster University, Hamilton, ON, Canada

<sup>f</sup> Department of Molecular & Biomedical Pharmacology, Sanders-Brown Center on Aging, University of Kentucky, Lexington, KY, USA

### Abstract

**Background**—Immune system activation is frequently reported in patients with Alzheimer's disease (AD). However, it remains unknown whether this is a cause, a consequence, or an epiphenomenon of brain degeneration.

**Objective**—The present study examines whether immunological abnormalities occur in a well-established murine AD model and if so, how they relate temporally to behavioral deficits and neuropathology.

**Methods**—A broad battery of tests was employed to assess behavioral performance and autoimmune/inflammatory markers in 3xTg-AD (AD) mice and wild type controls from 1.5 to 12 months of age.

**Results**—Aged AD mice displayed severe manifestations of systemic autoimmune/inflammatory disease, as evidenced by splenomegaly, hepatomegaly, elevated serum levels of anti-nuclear/anti-dsDNA antibodies, low hematocrit, and increased number of double-negative T splenocytes. However, anxiety-related behavior and altered spleen function were evident as early as 2 months of age, thus preceding typical AD-like brain pathology. Moreover, AD mice showed altered olfaction and impaired “cognitive” flexibility in the first 6 months of life, suggesting mild

\*Correspondence to: Boris Sakic, Ph.D., Department of Psychiatry and Behavioral Neurosciences, McMaster University, The Brain-Body Institute, St. Joseph's Healthcare T-3307, 50 Charlton Avenue East, Hamilton, Ontario, L8N 4A6, Canada. Tel.: +1 905 518 7833; Fax: +1 905 540 6593; sakic@mcmaster.ca..

#### AUTHOR CONTRIBUTIONS

Study conception, design, and diagrams: B.S. Data Acquisition: M.M., V.A., D.M., M.K., H. Z., P. D. Data Analysis, Graphics, and Interpretation: B.S, M.M., D. C., E.H., and K.K.

Authors' disclosures available online (<http://www.jalz.com/disclosures/view.php?id=1939>).

cognitive impairment-like manifestations before general learning/memory impairments emerged at an older age. Interestingly, all of these features were present in 3xTg-AD mice prior to significant amyloid- $\beta$  or tau pathology.

**Conclusion**—The results indicate that behavioral deficits in AD mice develop in parallel with systemic autoimmune/inflammatory disease. These changes antedate AD-like neuropathology, thus supporting a causal link between autoimmunity and aberrant behavior. Consequently, 3xTg-AD mice may be a useful model in elucidating the role of immune system in the etiology of AD.

### Keywords

Alzheimer's disease; amyloidosis; anxiety; autoimmunity; hepatomegaly; inflammation; mild cognitive impairment; olfaction; splenomegaly; 3xTg-AD model

## INTRODUCTION

Alzheimer's disease (AD) is an age-related, progressive neurodegenerative condition of unknown etiology. It is largely characterized by losses in multiple cognitive domains, psychiatric manifestations [1], and ultimately death within 9 years of diagnosis [2]. The lack of effective medication, prolonged life expectancy, and escalating incidence, has made AD a significant medical, social, and economic burden globally. According to the recent World Alzheimer's Report, more than 36 million people worldwide have been affected, with numbers expected to double every 20 years (<http://www.alz.co.uk/research/world-report-2012>). The neuropathological hallmarks of AD are extracellular deposits (plaques) of amyloid- $\beta$  peptide (A $\beta$ ) and filamentous intracellular aggregates (neurofibrillary tangles) of hyperphosphorylated tau protein [3]. Misfolded proteins, neuroinflammation [4, 5], oxidative stress [6], metal dysregulation [7], angiopathy [8], and neuronal death [9] are just some of the many pathogenic factors hypothesized to contribute to brain atrophy and neuropsychiatric manifestations. Similar to AD, amnesic mild cognitive impairment (aMCI) is an etiologically-unknown syndrome characterized by mild, age-independent deficits in one or more cognitive domains, but without the typical signs of significant functional decline indicative of AD [10]. Clinical studies have shown that subjects diagnosed with MCI are at increased risk to convert into AD (reviewed in [11]). Many patients with MCI present with spatial navigation deficits and impaired working and short-term memory, suggestive of early damage in the entorhinal-hippocampal circuitry [12]. Despite intact learning capacity, they perform poorly on a variety of tasks that require cognitive flexibility [13–15]. In particular, MCI patients have a tendency to adhere to previously learned responses, thus showing a high degree of perseveration. Similar to AD [16], deficits in executive function are often accompanied by depression, agitation, sleep disturbances, irritability, and anxiety (reviewed in [17]).

Prominent inflammatory and innate immune responses have been observed in both AD and MCI patients [18–20]. Initial evidence supporting an early, detrimental inflammatory process came from epidemiological studies showing that use of non-steroidal anti-inflammatory drugs (NSAIDs) among patients with rheumatoid arthritis is associated with a lower incidence of AD [21]. Postmortem analysis of brain tissue revealed that use of traditional NSAIDs correlated with fewer activated microglia [22]. Experimental studies

also demonstrated that administration of NSAIDs was accompanied by decreased microglial activation around plaques [23] and attenuation of A $\beta$  burden [24]. Although local inflammatory responses may accompany plaque formation, it remains unknown whether these immune mechanisms reflect a driving pathogenic force, bystander reaction, or reparative process [25].

So far, the peripheral immune systems of AD and MCI animal models have not been systematically explored in longitudinal studies. The triple-transgenic, 3xTg-AD (AD) substrain is one of several well-established murine models because it mimics several key aspects of AD neuropathology: 1) A $\beta$  plaques and neurofibrillary pathology develop in AD-relevant brain regions, such as the hippocampus, cortex, and amygdala; 2) plaque pathology precedes tangle formation, and plaques consist of the longer, more amyloidogenic A $\beta$  42; 3) the pattern of conformational and phosphorylation changes that the tau protein undergoes parallels the sequence in the human AD brain; 4) selective loss of nicotinic  $\alpha$ 7 receptors in the hippocampus and cortex [26–29]. In conjunction with an early, intra-neuronal accumulation of A $\beta$ , these mice also develop deficits in long-term potentiation, paired-pulse facilitation, and long-term memory [26, 30]. Being a commonly used animal model of AD, we tested the hypothesis that changes in the immune system develop alongside progressive behavioral dysfunction and emerging neuropathology.

## MATERIALS AND METHODS

### Animals

Given that tau-related pathology is comparable in both genders of AD mice [31] and that estrus cycling may confound assessment of disease-related behavioral dysfunction, males were used in the present project. The first cohort consisted of homozygous triple-transgenic AD mice possessing PS1<sub>M146V</sub>, A $\beta$ PP<sub>swe</sub>, and *tau*<sub>P301L</sub> transgenes and control, wild type (WT) mice ( $n = 20$  mice/genotype) purchased at 6 weeks of age. These mice were used for the longitudinal behavioral study in which immunological status was assessed at 12 months of age (i.e., when behavioral profiling was completed). Three AD mice died prematurely between 10 and 11 months of age, thus reducing the total sample size to  $N = 37$ . Considering significant discrepancies in the immune status were observed between the two phenotypes, a second cohort of 4 week-old males ( $n = 10$  mice/genotype) were purchased for a cross-sectional study to assess behavior and immune status before documented AD-like pathology (i.e., approximately 1.5 months of age). Upon arrival from the supplier (Jackson Laboratories, Bar Harbor, ME, USA), all mice were group-housed (4 mice/cage) and kept under standard laboratory conditions: light phase 7 A.M.-7 P.M., room temperature  $\sim 22^{\circ}\text{C}$ , humidity  $\sim 62\%$ , low fat rodent chow and tap water available *ad libitum*, and Beta Chip bedding changed twice a week. They were tail-tattooed with an ATS-3 tattoo machine (Animal Identification & Marking Systems Inc., <http://www.animalid.com>) and weighed on a weekly basis. All protocols were performed in accordance with the rules and regulations of the Canadian Council of Animal Care and approved by the local Animal Research Ethics Board.

## Behavioral testing

After acclimatization and 5-day habituation to experimenters, mice from the first cohort underwent a battery of behavioral tests at 3, 6, 9, and 12 months of age. The following measures and paradigms were used sequentially: 24-h food/water intake, Rota-Rod test, Morris water maze, spontaneous alternation behavior, brief sucrose preference test, step down test, olfactory preference, and novel object test. An identical behavioral battery was applied to mice in the second, younger cohort between the 7th-10th weeks of life.

**Food/water intake**—Daily food/water intake was estimated by individually housing mice over four days (in our experience, longer social isolation induces prolonged aggression among re-housed males). Food intake was measured as the difference in the weight of three food pellets (initial weight 11–14 g) left on the home-cage floor over 24 h. Water was provided in 150 ml leak-proof bottles and intake was quantified as the weight difference over a 24-h period.

**Rota-rod**—Sensorimotor coordination and motor learning were evaluated with the Rota-Rod apparatus (MedAssociates, Inc., St. Albans, VT). Mice were placed on top of a rotating drum (dia. = 3.2 cm, fall height, H = 16.5 cm), which gradually accelerated from 4–40 r.p.m. over 5 min. Mice were tested twice daily for fall latency across 3 days.

**Morris water maze (MWM)**—The MWM is a paradigm commonly used in the assessment of visuo-spatial learning and memory in rodents (reviewed in [32]). An 8-day MWM protocol was used to habituate the animals to the apparatus, assess their sensorimotor capacity, and examine their ability to form a spatial map. A transparent Plexiglas platform (dia. = 15 cm) was used as an escape from a polyethylene pool (dia. = 115 cm; H = 60 cm) filled with tap water (~24°C). To evaluate swimming ability and visual acuity, mice were trained in four 2-min trials to locate a visible platform cued with a black cylinder on Day 1 (Cue trials). The cue trial was considered completed when the mouse climbed onto the platform, or if 2-min expired. In case of failure, mice were guided to the platform and left to stay for ~60 s, as were mice that successfully located it. On Day 2, the platform was kept in the same location, but sub-merged and invisible. Blocks of acquisition trials (4 trials/day) were performed over the next four days. To examine whether a spatial learning strategy was employed in locating the platform, a 2-min probe trial was administered on Day 6. It was followed by 3 successive trials to evaluate the rate of response extinction. To assess “cognitive” flexibility, 4 cue reversal trials (Day 7) were followed by 4 acquisition reversal trials (Day 8). On each day, starting positions (North, South, East, and West) were randomly chosen. All behaviors were filmed with a ceiling video camera and scored for latency, speed, and distribution of swim paths with EthoVision XT4 tracking software (Noldus Information Technology, Leesburg, VA). The “thigmotactic area” (space along the inner side of the pool wall) was kept consistently at 16 cm.

**Spontaneous alternation behavior**—Spontaneous alternation behavior refers to the tendency of mice to alternate their non-reinforced choice of maze arms on successive trials. The test relies on a rodent's natural, unconditioned response to explore novel habitats and environmental stimuli. As the strategy inherently requires the animal to recognize which arm

of the maze they had previously explored, alternation rates have been commonly used to assess spatial learning and working memory [33]. The current study used the discrete-trial procedure, which has been shown to be sensitive to normal and pathological aging [34]. The T-maze, made of black Plexiglas, consisted of four perpendicular arms ( $H = 15 \text{ cm} \times L = 25 \text{ cm} \times W = 10 \text{ cm}$ ) and sliding doors that could modify the maze into an L, T, or + shape. Two sessions were given daily. Each session consisted of Trial 1 (5 s in a start position and entry into an unblocked arm), a 60 s inter-trial period (mouse restrained in the arm), and Trial 2, in which both arms were open, so the mouse could choose either the visited or unvisited arm after leaving the start position. An arm was considered to be chosen if all four limbs were within the arm. Following 5 days of acquisition trials, mice were run in a reversal trial on Day 6 to examine whether a spatial learning strategy was indeed employed. Trial 1 consisted of placing each mouse in the usual starting position. However, after a 60 s inter-trial period in the unblocked arm, Trial 2 was initiated from the arm located  $180^\circ$  from the starting position in Trial 1. If external spatial cues were used in memory formation, it was expected that the unvisited arm would be chosen by a body turn identical to Trial 1.

**Sucrose preference test**—Blunted responsiveness to palatable stimulation, as evidenced by reduced drinking of sucrose solutions, is proposed to model anhedonia, the second core symptom of depression [35]. The brief sucrose preference test was performed as described earlier [36, 37]. During the 3-day training, a plastic 10 ml syringe with 3 ml of 4% sucrose solution was attached to the cage lid. Following a 24-h sucrose free period, mice had brief access to 7 ml of 1, 2, 4, or 8% sucrose solutions, each being available between 9: 30–10: 30 P.M. in 1 out of 4 consecutive nights. The mass of sucrose ingested was used to calculate the dose-response curve.

**Step down test**—The step down test is designed to assess the readiness of a mouse to escape from an elevated platform by descending onto a firm, dark surface in a brightly-lit room [38, 39]. As such, it is proposed to evoke an anxiety-like response to height and/or bright lighting. Each mouse was gently placed in the center of a small platform ( $W = 10 \times L = 8 \text{ cm}$ ) made of wire-mesh, attached to the top of a 7 cm high rectangular Pyrex glass container. Latency to step down with all four paws was measured by a stopwatch (max. time 3 min).

**Olfactory tests**—These tests were used to compare responsiveness to different attractant and repellent olfactory cues. For the olfactory sensitivity tests, habituation to the experimental environment was achieved by placing a mouse into a transparent home cage 15-min prior to the trial. A  $5 \times 5 \text{ cm}$  piece of filter paper (Whatman Inc., Piscataway, NJ) scented with an odorant (250 J..1) was placed into the opposite corner. An attractant, Smooth peanut butter® (Kraft Canada Inc., North York, ON, dissolved in Exact Mineral Oil, Loblaw's Inc., Brampton, ON) and a repellent, Peppermint Essential Oil (Aura Cacia, Urbana, IA, dissolved in distilled water), were applied onto a filter paper at concentrations of 0.01, 0.1, 1, and 10%. To measure responsiveness to a neutral stimulus, a drop of water was applied onto a filter paper and introduced in a manner identical to both odorants. The length of each trial was 3-min. Mice were exposed to a single concentration on each testing day. Testing cages were covered with a clear piece of Plexiglas to limit evaporation and

entry of external odors. Behavioral performance was digitally recorded and scored by an unbiased experimenter using Observer XT software (Noldus). Active investigation was defined as directed sniffing within 0.5 cm of the odor source. After each trial, mice were returned to their home-cage, while the experimental cage was cleaned with Quatricide® disinfectant. In addition to the above tests, the response to a salient odor (pellets of Cap'n Crunch cereal) was used to examine whether AD mice develop a loss of smell (anosmia). We employed the buried food pellet test, a paradigm proposed to rely on a rodent's intrinsic tendency to follow olfactory cues when foraging [40, 41]. Latency to locate a pellet of buried cereal was measured in food-deprived mice over four trials (1 trial/day). The detailed protocol is described in our recent report [42].

**Novel object test**—Performance in the novel object test is proposed to reflect exploratory and emotional responses in an approach-avoidance situation [38]. Mice were permitted to explore an arena ( $W = 45 \times L = 45 \times H = 20$  cm) for 5 min before a small pyramid was positioned in the center of the field for an additional 5 min. Latency to approach the object, contact frequency, and duration of direct contact with the object were quantified using EthoVision XT 7 software and 3-point detection module (Noldus Information Technology). In addition, distance traversed, velocity, and the ratio of time spent in the center versus periphery were analyzed in “empty” (no novel object in the arena) and “full” (novel object present in the arena) phases. Following each session, the arena was cleaned and disinfected with Quatricide®.

### Systemic manifestations

Mice were anesthetized with an i.p. injection of a ketamine/xylazine mixture at 12 months (the first, older cohort) and ~1.5 months of age (the second, younger cohort).

**Serum autoantibody levels**—Blood (~1 ml) was collected from the i.p. cavity within 15 s of severing the vena cava. Using a MasterFlex® peristaltic pump, blood vessels were intracardially perfused with ~120 ml of phosphate buffered saline over 5 min. Extracted spleens, livers, kidneys, and brains were wet weighed on a Sartorius 2024 MP analytical scale (VWR Scientific, Canada).

Anti-nuclear antibody (ANA) levels were measured using a fully-automated IFA system (IF Sprinter). Sera were diluted to 1 : 80 in PBS buffer (pH 7.2) and 30  $\mu$ l of the diluted serum was pipetted into the corresponding well of HEp-2 cell slides (EUROIMMUN). The slides were washed 4 times using PBS-Tween20 after 30 min of incubation at room temperature. Thirty  $\mu$ l of 1 : 100 diluted rabbit anti-mouse IgG-FITC conjugate (Sigma-Aldrich) was pipetted into each well. The slides were washed again as above after 30-min incubation with the conjugate. Using 10  $\mu$ l of the mounting medium, the slides were sealed with a cover glass. The results were obtained by viewing slides under a LED-fluorescence microscopy (EUROStar III). Serum levels of anti-dsDNA autoantibodies were quantified using a fully automated ELISA analyzer (EUROIMMUN Analyzer I). Briefly, 100  $\mu$ l of each sample (serum 1 : 50 dilution in sample buffer) was transferred into the corresponding microtiterplate well (EUROIMMUN pre-coated microtiterplate). Each well contained antigen substrate of dsDNA complexed with nucleosomes and coupled to the solid phase.

Each sample was incubated for 30 min at room temperature and then washed three times with 450  $\mu$ l of working strength wash buffer. One hundred microliters of 1 : 2000 diluted rabbit anti-mouse IgG-HRP conjugate (Promega) was pipetted into each of the microtiterplate wells, left to incubate, and washed to remove unbound HRP enzyme conjugate. Subsequently, 100  $\mu$ l of chromogen/substrate solution (3,3',5,5'-tetramethylbenzidine) was pipetted into each well of the microtiterplate and incubated for another 20 min at room temperature. One hundred microliters of stop solution was added to each well in the same order and at the same speed as when the chromogen/substrate solution was introduced. The microtiterplate was shaken at a speed of 20 Hz for 5 s to ensure a homogeneous distribution of the solution. Optical density was determined at a wavelength of 450 nm and a reference wavelength of 620 nm within 10 min of adding the stop solution. Observed results are expressed as relative optical densities.

**Hematocrit**—Retro-orbital blood samples were taken with heparinized Fisher microhematocrit capillary tubes. The Standard Adams method was used to measure hematocrit, as described earlier [43]. Briefly, sealed tubes were centrifuged for 10 min in a standard microhaema-tocrit centrifuge (Clay-Adams, Parsippany, NJ) and read in a Critocaps reader. Low hematocrit (<40%) is often used as a measure of hemolytic anemia [44].

**T splenocyte distribution**—The spleen contains a large number of immune cells, including CD4+ and CD8+ T cells [45]. The distribution of splenic lymphocyte subsets is different from peripheral blood, implying a distinct role of the spleen in CD4+ and CD8+ T cell activation [46]. Considering the spleen is an important organ in the bi-directional communication between the nervous and immune systems [47, 48], we selected splenocytes to investigate the pathologic factors in neuroinflammation. Splenocyte suspensions were prepared and analyzed by flow cytometry, as described earlier [49, 50]. Splenocytes were re-suspended in FACS buffer (PBS-1% fetal calf serum) and stained for surface markers CD3 (BD Pharmingen, San Diego, CA), CD4, and CD8 (eBio-sciences, San Diego, CA). Data were acquired with Becton Dickinson flow cytometer (Oakville, Canada) and analyzed with FlowJo program (TreeStar, Ashland, OR).

## Neuropathology

4% Paraformaldehyde-fixed sections were sent to Neuroscience Associates (<http://www.neuroscienceassociates.com/>, Knoxville, TN) to be cut serially. The right hemisphere was embedded in a gelatin matrix, serial coronal sections were cut at 40  $\mu$ m, and placed in an antigen preserving solution (PBS, ethylene glycol, and poly-vinyl-pyrrolidone) for long-term storage at  $-20^{\circ}\text{C}$ . Free floating sections containing the hippocampus were selected for analysis, using immunohistochemical techniques described previously [51]. In brief, sections were stained for A $\beta$  plaques (6E10, Covance, Emeryville, CA, 1 : 2000; A $\beta$  1-42, Invitrogen, Carlsbad, CA, 1 : 500), or phosphorylated tau (pSer202/Thr205) (AT8, Thermo Scientific, Rockford, IL, 1 : 10,000). When staining for A $\beta$  plaques, a pre-treatment was done in 90% formic acid for 3 min [52]. Following an overnight incubation at room temperature in primary antibody, the tissue was incubated in biotinylated secondary antibody (Vector Laboratories, Burlingame, CA). For mouse primary monoclonal



antibodies, a Mouse on Mouse kit (Vector Laboratories) was used. After several washes, sections were incubated for 1 h in an avidin-biotin complex and detection was accomplished by 3,3'-diaminobenzidine and hydrogen peroxide, DAB (Vector Laboratories). To characterize AT8 in the hippocampus, photos were taken for each animal at 20 $\times$ . Two independent investigators, blind with respect to the group, characterized immunostaining as 1 (no or little neuronal staining); 2 (scattered immunopositive neurons); 3 (extensive neuronal staining). An endstage AD case was included in all experiments as a positive control for both 6E10 and AT8 experiments.

### Statistical analysis

Raw data were analyzed using SPSS 20 software package (SPSS Inc., Chicago, IL). Analysis of variance (ANOVA) was used in the overall analysis, with Group and Age as between-group factors, and Trial or Concentration as within-group factors, when applicable. If significant interactions were detected, Student's *t*-test was used in post-hoc comparisons. Linear relationships between scale variables were analyzed by Pearson's and Spearman's correlations. The significance level was set at  $p = 0.05$  in two-way comparisons. Graphs indicate mean values  $\pm$  SEM, with significant differences of  $p = 0.05$ ,  $p < 0.01$ , and  $p < 0.001$ , shown as \*, \*\*, and \*\*\*, respectively. To simplify graphical presentation of individual measures, results from both age cohorts are shown on single line graphs, instead of separate bar graphs.

## RESULTS

### Body and organ weights

All measures of body and organ weights collected at sacrifice are shown in Table 1. As expected, both AD and WT mice gained weight (Age:  $F_{1,53} = 217.807$ ,  $p < 0.001$ ), suggesting an absence of malnutrition during the study. However, AD males from the younger and the older cohort were ~11-12% lighter than age-matched WT controls (Group:  $F_{1,53} = 17.541$ ,  $p < 0.001$ ). Similarly, brain weight increased with age in all mice (Age:  $F_{1,53} = 19.388$ ,  $p < 0.001$ ), but was consistently ~9-10% lower in AD mice, in comparison to the WT groups (Group:  $F_{1,53} = 40.771$ ,  $p < 0.001$ ). The lack of significant positive correlations between body mass and brain mass (for AD group  $r_{16} = -0.08$ , n.s.) suggested that the lower brain weight is not directly associated with lower body weight. Although mass of kidneys and liver were comparable, spleens were heavier in 2 month-old AD mice than in age-matched controls ( $t_{18} = 2.339$ ,  $p = 0.031$ ). This early, yet moderate enlargement in the AD group culminated in splenomegaly at 12 months, with spleens ~10–30-fold heavier than in the age-matched WT group (shown on Fig. 4A), or when compared to the young AD cohort (Group by Age:  $F_{1,53} = 18.834$ ,  $p < 0.001$ ). Although the weight of kidneys was comparable at 12 months, liver mass increased in the AD group, suggesting the development of age-dependent hepatomegaly in the AD group (Group by Age:  $F_{1,53} = 6.613$ ,  $p = 0.013$ ; Table 1). Similarly, unilateral enlargement of the adrenal gland was observed exclusively in the group of aged AD mice (Group by Side:  $F_{1,30} = 4.846$ ,  $p = 0.036$ ; Table 1). Taken together, the obtained results pointed to age-dependent splenomegaly, hepatomegaly, and hyperplasia of the right adrenal gland in AD mice, without signs of generalized organ enlargement.

## Behavior

**Ingestive behavior**—Although daily intake of standard mouse chow was relatively constant in the control WT group (~3-4 g/day), it increased in 6-month old AD mice (Group by Age:  $F_{3,186} = 5.664$ ,  $p = 0.001$ ). This coincided with higher daily water intake (~5-7 ml) in AD mice, but group discrepancies were likely attributable to diminished water consumption by WT mice (Group by Age:  $F_{3,186} = 3.374$ ,  $p = 0.022$ ). These differences suggested altered metabolic demands in aging AD mice.

**Morris water maze**—Detailed group performance in the MWM is summarized in Fig. 1. When the platform was visible in cued trials (Days 1 and 7), all groups showed comparable latency to climb the platform. This suggested that AD mice have no deficits in regards to visual acuity and swimming capacity. However, when the platform was submerged, there was a trend for a longer escape latency in the 1.5 month-old AD group (Group:  $F_{1,18} = 9.28$ ,  $p = 0.054$ ). This was associated with higher swimming speed and increased thigmotaxis (swimming along the pool walls) in AD mice on specific response acquisition days [e.g., Day 2, Speed: ( $t_{18} = 2.539$ ,  $p = 0.021$ ), Thigmotaxis time ( $t_{18} = 2.516$ ,  $p = 0.022$ )]. A similar response, characterized by prolonged latency, faster swimming, and increased thigmotaxis, was observed when a separate cohort of 2.5 month-old AD mice was tested on Acquisition Day 1 [Group by Day: Latency  $F_{3,108} = 6.13$ ,  $p < 0.001$ ; Speed ( $t_{36} = 3.734$ ,  $p < 0.001$ ); Thigmotaxis ( $t_{36} = 2.073$ ,  $p = 0.045$ )]. Although a similar response was not seen at later time points, the AD group generally showed slower rate of acquisition response than the control group when tested at 6, 9, and 12 months of age (Group by Day:  $F_{3,180} = 3.515$ ,  $p = 0.018$ ). No significant group differences were observed in the probe trial, suggesting that all cohorts located the platform using spatial strategy. Response extinction was comparable between the 1.5 month-old groups, with AD mice unexpectedly spending less time in the target quadrant in one trial (Group by Trial:  $F_{2,36} = 3.362$ ,  $p = 0.046$ ). However, this changed in the opposite direction in older AD mice: their response extinction rate was consistently slower than in the control group (Group by Trial:  $F_{2,180} = 3.403$ ,  $p = 0.04$ ). When the escape platform was moved to the opposite quadrant and remained visible, all cohorts promptly mounted it. As seen in the initial acquisition trials, AD mice at 2.5 and 12 months demonstrated an increased latency to locate the platform in the opposite quadrant (Group:  $F_{1,30} = 13.46$ ,  $p < 0.001$ ). A Group by Age trend ( $F_{3,90} = 2.405$ ,  $p = 0.073$ ), and visual inspection of Fig. 1 suggest that this deficit fluctuates during aging and/or disease development in AD mice. Nevertheless, this deficit was largely accounted for by their perseverative response, as evidenced by prolonged time spent in the previous goal quadrant (Group:  $F_{1,30} = 7.847$ ,  $p < 0.01$ ; Group by Age trend  $F_{3,90} = 2.46$ ,  $p = 0.068$ ). Taken together, the above results suggested an enhanced emotional response in young AD mice when the escape platform is hidden, as well as slower response acquisition rate, slower extinction, and enhanced perseveration (“cognitive” inflexibility) from 6 months of age.

**Rota-rod**—Longer fall latencies in both cohorts exposed to successive Rota-Rod trials suggested an improved and comparable performance across all groups (Trials:  $F_{5,450} = 33.37$ ,  $p < 0.001$ ; data not shown). The lack of significant group differences at all ages (Fig. 2A) suggested that sensorimotor coordination in the AD groups was comparable to the controls.

**Spontaneous alternation behavior**—Comparable mean spontaneous alternation rates (~66 versus 73%,  $\chi^2 = 2.486$ , n.s.) were observed at 1.5 months. However, at all older ages, the spontaneous alternation behavior rate was consistently ~10% lower in the AD group than in the controls, most often around 55% (Group:  $F_{1,30} = 9.28$ ,  $p = 0.005$ ; Fig. 2B). Reversal trials did not reveal any group differences throughout the study, confirming that all cohorts used spatial strategy and not local cues. Taken together, these results pointed to an early and steady deficit in the formation of spatial memory in the AD group starting at 3 months of age.

**Sucrose preference test**—No group differences were observed in the brief sucrose preference test, suggesting that the responsiveness to palatable stimulation was normal in the AD groups.

**Step down test**—Consistent with the notion of increased anxiety-like behavior, AD groups showed prolonged latency to step-down from an elevated platform at both young (Group:  $t_{18} = 2.156$ ,  $p = 0.045$ ) and older ages (Group:  $F_{1,30} = 10.309$ ,  $p = 0.003$ ; Fig. 2C). The results observed in both cohorts suggested a sustained, enhanced fear of heights/bright lighting in the AD group.

**Novel object test**—No significant group differences were detected when young, 1.5 month-old mice were exposed to the novel object test. However, after 9 months of age, AD mice travelled shorter distances in the arena devoid of the object (Group:  $F_{1,29} = 6.042$ ,  $p = 0.02$ ). Although they explored novel objects and moved at a speed comparable to WT mice (data not shown), their latency to approach the object increased significantly at 12 months of age (Group:  $t_{20} = 3.108$ ,  $p = 0.006$ , Fig. 2D).

**Olfactory function**—No significant group differences in sniffing duration were observed when papers with different concentrations of peppermint were placed into the cage (data not shown). Similarly, both groups spent comparable time exploring filter papers soaked in water, or scented with increasing concentrations of peanut butter at 1.5 months of age (first data point on Fig. 3A–E). With aging, both AD and WT mice increased investigation of filter paper impregnated with peanut butter (Age:  $F_{3,270} = 24.559$ ,  $p < 0.001$ ; Fig. 3B–E). However, this increase was more profound in AD mice at all concentrations (Group by Age:  $F_{3,270} = 7.662$ ,  $p < 0.001$ ). This discrepancy did not seem to reflect impaired sensory input considering AD mice located the buried food pellet faster than controls starting at 6 months of age (Group by Age  $F_{3,261} = 5.143$ ,  $p = 0.003$ ; data not shown). In summary, when exposed to an olfactory attractant, AD mice show age-dependent alterations in olfactory function.

Collectively, the above behavioral results suggested an early development of enhanced emotional reactivity, which was detected in several paradigms from 1.5 month to 12 months of age (e.g., increased thigmotaxis in the MWM, prolonged latency to descend in the step-down test, increased latency to approach a novel object). This “timid” behavioral profile developed in parallel with MCI-like changes in behavior before 6 months of age, as reflected by altered olfactory function and fluctuating “cognitive” flexibility. More generalized

deficits in response acquisition and learning/memory performance appeared around 12 months of age.

### Immunopathology

**FACS analysis**—In addition to spleen enlargement (Fig. 4A), profound changes in splenic T cell populations were observed in AD mice (representative dot plots are shown in Fig. 4B). Although group discrepancies differed in magnitude, they were observed at both 2 and 12 months of age (Fig. 4C). In the young cohort, subtle, but significant group differences were noted, including less CD3<sup>+</sup> ( $t_8 = 2.439$ ,  $p = 0.041$ ), CD4<sup>+</sup> CD8<sup>-</sup> ( $t_8 = 2.771$ ,  $p = 0.024$ ), and CD4<sup>+</sup> CD8<sup>+</sup> splenocytes ( $t_8 = -3.437$ ,  $p = 0.009$ ) in AD mice.

However, more CD4<sup>-</sup>CD8<sup>-</sup> splenocytes were seen in 2 month-old AD mice, than in age-matched WT controls ( $t_8 = -2.237$ ,  $p = 0.045$ ). This skewed ratio between CD<sup>+</sup> and double negative subpopulations was exacerbated in the 12 month-old groups. This was evidenced by an enhanced reduction in the number of CD3<sup>+</sup> (Group by Age:  $F_{1,12} = 39.252$ ,  $p < 0.001$ ), CD4<sup>+</sup> CD8<sup>-</sup> (Group by Age:  $F_{1,12} = 31.716$ ,  $p < 0.001$ ), CD4<sup>+</sup> CD8<sup>+</sup> (Group by Age:  $F_{1,12} = 9.871$ ,  $p = 0.009$ ), and CD4<sup>-</sup>CD8<sup>+</sup> cells (Group by Age:  $F_{1,12} = 57.355$ ,  $p < 0.01$ ).

Conversely, the sub population of CD4<sup>-</sup> CD8<sup>-</sup> increased further in the aged AD group (Group by Age:  $F_{1,12} = 52.92$ ,  $p < 0.01$ ). Overall, the subpopulation of CD4<sup>-</sup>CD8<sup>-</sup> splenocytes expanded in young AD mice at the expense of CD<sup>+</sup> clones and became more abundant with age.

**Serological measures**—While no young WT controls showed ANA staining, serum samples from 50% of ~2-month old AD mice showed either nuclear (3/5), homogenous (1/5), or cytoplasmic (1/5) staining pattern (Fisher's Exact test,  $p = 0.032$ ; Fig. 5A). Although the intensity of staining increased in the older AD group, this difference was less profound because 75% of aged WT controls had developed similar reactivity, ranging from very weak to strong. Compared to this qualitative assessment, quantification of anti-dsDNA antibodies by ELISA revealed significantly higher serum levels in AD mice, both at 2 and 12 months of age (Group:  $F_{1,48} = 6.35$ ,  $p = 0.015$ , Fig. 5B). Interestingly, serum levels of anti-dsDNA antibodies increased with age in both groups (Age:  $F_{1,48} = 4.695$ ,  $p = 0.035$ ). While there were no significant differences in hematocrits of young cohorts (45–47%), the values dropped significantly in aged AD mice, in some cases, as low as 20% (Group by Age:  $F_{1,43} = 42.364$ ,  $p < 0.001$ , Fig. 5C). In the context of increased levels of autoantibodies in serum, the latter result suggested development of autoimmune hemolytic anemia in aged AD mice.

### Neuropathology

To detect A $\beta$  pathology in mice, sections were immunostained using 6E10 (A $\beta$ <sub>1-16</sub>) after formic acid pretreatment to optimize detection. The AD positive control case showed extensive A $\beta$  accumulation (Fig. 6A). However, little or no plaque labeling was noted in 3xTg-AD or WT mice at 12 months of age (Fig. 6C, E, respectively). Expectedly, no A $\beta$  was detected in 2 month-old WT mice (data not shown).

AT8 labeling in the AD case revealed significant intra-cellular neurofibrillary tangle formation (Fig. 6B), but was comparable in 12 month-old 3xTg-AD and WT mice (Fig. 6D, F, respectively), which was further similar to 2 month-old AD mice (Fig. 6G). Higher magnifications showed sporadic neuronal labeling, which did not appear to resemble neurofibrillary tangles (Fig. 6H).

## DISCUSSION

The present study tested the possibility that immunological changes parallel behavioral deficits and neuropathology in 3xTg-AD mice. The obtained results support previous evidence on age-dependent behavioral dysfunction, largely in domains of emotional reactivity and learning/memory capacity. Although olfactory function in AD mice changed significantly with aging, visual acuity and sensorimotor capacity did not seem to be affected, as measured by performance in cue trials, Rota-rod test, or walking/swimming speed. Early changes in anxiety-related behaviors appear as distinct prodrome to age-related decline in learning/memory performance. In the first 6 months of life, AD mice show MCI-like changes, as suggested by enhanced emotional reactivity (e.g., “acrophobia” in the step-down test, “neophobia” in the novel object test), altered olfactory function, and impairments in “cognitive” flexibility when tested in the reversal trials of the water maze. Between 6 and 12 months of age, more complex performance deficits in learning/memory tasks are accompanied by severe manifestations of systemic autoimmunity and inflammation. The kinetics of responses suggests that behavioral and immunopathological manifestations in AD mice are not inbred. More interestingly, changes in the immune system and behavioral performance emerge well before the expected appearance of intra-neuronal damage and extracellular deposits [30]. Early alterations in immune status are reminiscent of systemic autoimmune/inflammatory disease accompanied by amyloidosis.

Similar to our results, neither learning/memory deficits, nor brain pathology were apparent in 3xTg-AD mice at 2 months of age [30]. The deficit in reversed water maze task at 2.5 months of age manifested as an inability to retain day-to-day information, without signs of an overall impairment in learning. Such dysfunction was proposed to resemble human aMCI, in which episodic memory is affected, but other cognitive processes are largely maintained [53]. Along the same line, significant impairments in attention are documented in AD patients and mice [54]. As we observed in the “reversal” trials, AD mice attend less accurately to spatial stimuli when the attentional demand of the task was increased, likely accounting for more perseverative responses. Enhanced anxiety-like behavior in our young AD cohort is consistent with enhanced deflection [55] and high swimming navigation speed [56]. This notion of increased anxiety is further supported by the evidence of early enhancements in innate-and conditioned-fear responses [57]. Along the same line, group-housed 6 month-old 3xTg-AD mice showed enhanced acoustic startle response, reduced locomotion in the open-field, and impaired spontaneous alternation in the Y-maze [58]. As in our water maze, they showed normal retention and “cognitive” impairment limited to the Y-maze test.

As we observed in aged males, aged AD females exhibit a higher level of fear and anxiety, demonstrated by increased restlessness, startle responses, and freezing behaviors [59].

Moreover, the same study could not detect differences between AD and WT mice with respect to muscle strength and visuo-motor coordination. Lastly, altered response to an attractant scent in AD mice is consistent with reported deficits in odor-based memory formation [60]. This deficit may be conceptually related to the early olfactory deficits in MCI patients [61], who are at particular risk to develop AD [62, 63]. Taken together, the current behavioral model is consistent with previous observations and interpretations. As such, it appears valid and comparable to an MCI-like stage of progression.

In the first studies of aged AD mice, intracellular A $\beta$  was observed at 4 months of age in the hippocampus, cortex, and amygdala, without extracellular AB deposits in plaques [30]. At 6 months, extracellular A $\beta$  plaques in the cerebral cortex and intracellular A $\beta$  accumulation were seen within pyramidal neurons of the CA1 region, baso-lateral amygdala, and cortical neurons. Typically, AD mice show intracellular phosphorylated tau accumulation after 12 months of age. In the current study, they did not show AB plaque accumulation or significant tau phosphorylation. We did observe sporadic neurons positive for AT8, but no systematic differences with age or genotype were observed, suggesting this signal was not disease-dependent. The current lack in neuropathology is consistent with delayed disease progression in males [64], relatively mild AD-like neuropathology at 12 months [31], and appearance of extracellular A $\beta$  1-42 plaques after 15 months of age [65]. Taken together, the neuropathological data suggested a shift to later ages in this mouse line. Alternatively, one may hypothesize that extensive behavioral testing lead to a reduction in AD neuropathology, as shown in this [66, 67] and other mouse models of AD [68–70].

Several lines of evidence suggest that chronic inflammation [71] and autoimmunity are associated with AD pathogenesis [72, 73]. More recently, it was shown that chronic peripheral inflammation in 3xTg-AD [74] and even WT mice promotes AD-like neuropathology [75]. The notion of sustained inflammatory response in AD-like disease is consistent with the evidence that “double-negative” T cells produce pro-inflammatory cytokines [76, 77]. However, hemolytic anemia, increased levels of serum autoantibodies, and increased number of double-negative T lymphocytes in the aged cohort of AD mice also suggest an insidious, ongoing autoimmune process. In addition to elevated levels of circulating autoantibodies, an increase in double CD-negative population is characteristic of systemic autoimmune conditions [78], such as multiple sclerosis [79], as well as human and murine forms of lupus erythematosus [80, 81]. Along the same line, hepatomegaly and splenomegaly (seen in our aged AD cohort) are common manifestations of amyloidosis. Although the cause of primary amyloidosis in humans is unknown, one may hypothesize that transfer of human antigens to produce the 3xTg-AD model accelerated this process in mice. Since amyloidosis is often associated with excess production of antibodies, in the case of the 3xTg-AD model, it may have induced an autoimmune response accompanied by inflammation. Several etiological factors may account for aberrant behavior in AD-like disease (Fig. 7). They may involve a cascade of various insults, starting with aging, genetic abnormality (here induced by the transfer of human genes), and environmental insults (Fig. 8). In the 3xTg-AD model, one may hypothesize that resulting amyloidosis in the spleen and liver may induce systemic inflammatory/immune responses which compromise the integrity of the blood-brain barrier. Increased permeability of the blood-brain barrier may facilitate the entry of autoantibodies into the CNS and promote disintegration of neuronal

microtubules, ultimately leading to the formation and deposition of neurofibrillary tangles. The ensuing CNS inflammation, neuronal death, and disturbed neurotransmission may functionally result in diverse behavioral deficits. The immunological changes observed in young AD mice are consistent with clinical evidence on increased production of the pro-inflammatory cytokine TNF- $\alpha$  and decreased production of the anti-inflammatory cytokine TGF- $\beta$  in patients with MCI at risk to develop AD, jointly suggesting that inflammation is an early hallmark in the pathogenesis of AD [20]. In addition, serum levels of anti-A $\beta$  and anti-RAGE autoantibodies are several times higher in AD patients, showing positive correlation with cognitive dysfunction [82]. Consistent with these findings, anti-A $\beta$  antibodies were documented in AD patients [83] and aged A $\beta$  PP mice with AD-like neuropathology [84]. Moreover, serum from these mice potentiated the neurotoxicity of A $\beta$ , prompting the authors to suggest that humoral immune responses may promote neuronal degeneration [84]. Along the same lines, significant increase in parenchymal immunoglobulin-labeling of degenerating neurons in the entorhinal cortex and hippocampus of AD brains points to the presence of anti-neuronal autoantibodies [85].

Although anatomical asymmetry in adrenal gland innervation has been documented in rodents [86], increased mass of the right adrenal gland in aged AD mice is an unexpected observation. However, it may be consistent with the evidence that 3xTg-AD mice exhibit an early activation of the hypothalamic-pituitary-adrenal axis, as evidenced by altered mRNA levels of glucocorticoid receptors and corticotropin-releasing hormone in various parts of the limbic system [87]. These hormonal changes coincide with early-stage neuropathology and mild behavioral deficits, suggesting ongoing neuroendocrine alteration before the emergence of severe AD-like pathology and learning/memory deficits.

Despite the wealth of behavioral and immunological measures collected in the current study, it is not clear whether early inflammatory/autoimmune manifestations cause behavioral dysfunction or reflect epiphenomena to an incipient disease process in AD mice. To address this issue of causality, the logical step forward would include investigating whether generalized suppression of the immune system attenuates systemic disease and prevents behavioral deficits in the 3xTg-AD model. Similarly, the etiology of reduced brain weight in the AD group remains unknown. Lack of positive correlation with lower body weight would suggest that the brains of AD mice undergo *bona fide* neurodegeneration, but this notion seems premature without a time-course and morphometric assessment of cortical thickness, brain and ventricle area, as well as, hippocampal size. Future studies are also needed to confirm amyloidosis (e.g., Congo-red staining of liver and spleen), and hypothalamic-pituitary-adrenal axis activation (e.g., corticotropin-releasing hormone and corticosterone levels) to support the aforementioned pathogenic mechanisms.

Collectively, autoimmune-like changes, as evidenced by splenomegaly, emergence of double-negative T cells, increased serum levels of anti-dsDNA antibodies, and reduced hematocrit, suggest an early development of immunological dysfunction in 3xTg-AD mice. More interestingly, they antedate overt AD-like brain pathology and coincide with behavioral changes, implying a cause-effect relationship between autoimmunity and behavioral dysfunction. These findings point to a novel use for the 3xTg-AD model in testing the neuroimmunological circuits in AD etiology. Importantly, the results point to the

possibility that AD pathogenesis should be broadened beyond the context of CNS-centered disease involvement by exploring systemic manifestations in peripheral tissues and organs.

## ACKNOWLEDGMENTS

This project was funded by operating, equipment, and personal grants from Ontario Mental Health Foundation, Hamilton Health Sciences Foundation, Scottish Rite, and March of Dimes (Hamilton Chapter) to Drs. B. Sakic, D. Cowan, and M. Marchese. We are thankful to Yitian Ma at EuroImmun Canada (Mississauga, ON) for assistance with ELISA assays and Mrs. Rupal Hatkar with scoring of olfactory tests.

## REFERENCES

1. Diniz BS, Butters MA, Albert SM, Dew MA, Reynolds CF III. Late-life depression and risk of vascular dementia and Alzheimer's disease: Systematic review and meta-analysis of community-based cohort studies. *Br J Psychiatry*. 2013; 202:329–335. [PubMed: 23637108]
2. Querfurth HW, LaFerla FM. Alzheimer's disease. *N Engl J Med*. 2010; 362:329–344. [PubMed: 20107219]
3. Selkoe DJ. Alzheimer's disease: Genes, proteins, and therapy. *Physiol Rev*. 2001; 81:741–766. [PubMed: 11274343]
4. McGeer EG, McGeer PL. Neuroinflammation in Alzheimer's disease and mild cognitive impairment: A field in its infancy. *J Alzheimers Dis*. 2010; 19:355–361. [PubMed: 20061650]
5. Wyss-Coray T, Mucke L. Inflammation in neurodegenerative disease—a double-edged sword. *Neuron*. 2002; 35:419–432. [PubMed: 12165466]
6. Reddy VP, Zhu X, Perry G, Smith MA. Oxidative stress in diabetes and Alzheimer's disease. *J Alzheimers Dis*. 2009; 16:763–774. [PubMed: 19387111]
7. Adlard PA, Bush AI. Metals and Alzheimer's disease. *J Alzheimers Dis*. 2006; 10:145–163. [PubMed: 17119284]
8. Honjo K, Black SE, Verhoeff NP. Alzheimer's disease, cerebrovascular disease, and the beta-amyloid cascade. *Can J Neurol Sci*. 2012; 39:712–728. [PubMed: 23227576]
9. Yankner BA. Mechanisms of neuronal degeneration in Alzheimer's disease. *Neuron*. 1996; 16:921–932. [PubMed: 8630250]
10. Petersen RC, Smith GE, Waring SC, Ivnik RJ, Tangalos EG, Kokmen E. Mild cognitive impairment: Clinical characterization and outcome. *Arch Neurol*. 1999; 56:303–308. [PubMed: 10190820]
11. Petersen RC. Mild cognitive impairment as a diagnostic entity. *J Intern Med*. 2004; 256:183–194. [PubMed: 15324362]
12. Hort J, Laczó J, Vyhňalek M, Bojar M, Bures J, Vlcek K. Spatial navigation deficit in amnesic mild cognitive impairment. *Proc Natl Acad Sci U S A*. 2007; 104:4042–4047. [PubMed: 17360474]
13. Arnaiz E, Almkvist O. Neuropsychological features of mild cognitive impairment and preclinical Alzheimer's disease. *Acta Neurol Scand Suppl*. 2003; 179:34–41. [PubMed: 12603249]
14. Ready RE, Ott BR, Grace J, Cahn-Weiner DA. Apathy and executive dysfunction in mild cognitive impairment and Alzheimer disease. *Am J Geriatr Psychiatry*. 2003; 11:222–228. [PubMed: 12611752]
15. Nagahama Y, Okina T, Suzuki N, Matsuzaki S, Yamauchi H, Nabatame H, Matsuda M. Factor structure of a modified version of the wisconsin card sorting test: An analysis of executive deficit in Alzheimer's disease and mild cognitive impairment. *Dement Geriatr Cogn Disord*. 2003; 16:103–112. [PubMed: 12784035]
16. Jost BC, Grossberg GT. The evolution of psychiatric symptoms in Alzheimer's disease: A natural history study. *J Am Geriatr Soc*. 1996; 44:1078–1081. [PubMed: 8790235]
17. Apostolova LG, Cummings JL. Neuropsychiatric manifestations in mild cognitive impairment: A systematic review of the literature. *Dement Geriatr Cogn Disord*. 2008; 25:115–126. [PubMed: 18087152]



18. Wyss-Coray T, Rogers J. Inflammation in Alzheimer disease—a brief review of the basic science and clinical literature. *Cold Spring Harb Perspect Med.* 2012; 2:a006346. [PubMed: 22315714]
19. Trollor JN, Smith E, Baune BT, Kochan NA, Campbell L, Samaras K, Crawford J, Brodaty H, Sachdev P. Systemic inflammation is associated with MCI and its subtypes: The Sydney Memory and Aging Study. *Dement Geriatr Cogn Disord.* 2010; 30:569–578. [PubMed: 21252552]
20. Tarkowski E, Andreasen N, Tarkowski A, Blennow K. Intrathecal inflammation precedes development of Alzheimer's disease. *J Neurol Neurosurg Psychiatry.* 2003; 74:1200–1205. [PubMed: 12933918]
21. McGeer PL, McGeer E, Rogers J, Sibley J. Anti-inflammatory drugs and Alzheimer disease. *Lancet.* 1990; 335:1037. [PubMed: 1970087]
22. Mackenzie IR. Anti-inflammatory drugs and Alzheimer-type pathology in aging. *Neurology.* 2000; 54:732–734. [PubMed: 10680812]
23. Van Groen T, Kadish I. Transgenic AD model mice, effects of potential anti-AD treatments on inflammation and pathology. *Brain Res Brain Res Rev.* 2005; 48:370–378. [PubMed: 15850676]
24. Lim GP, Yang F, Chu T, Chen P, Beech W, Teter B, Tran T, Ubeda O, Ashe KH, Frautschy SA, Cole GM. Ibuprofen suppresses plaque pathology and inflammation in a mouse model for Alzheimer's disease. *J Neurosci.* 2000; 20:5709–5714. [PubMed: 10908610]
25. Aguzzi A, Barres BA, Bennett ML. Microglia: Scapegoat, saboteur, or something else? *Science.* 2013; 339:156–161. [PubMed: 23307732]
26. Oddo S, Caccamo A, Shepherd JD, Murphy MP, Golde TE, Kaye R, Metherate R, Mattson MP, Akbari Y, LaFerla FM. Triple-transgenic model of Alzheimer's disease with plaques and tangles: Intracellular A $\beta$  and synaptic dysfunction. *Neuron.* 2003; 39:409–421. [PubMed: 12895417]
27. Oddo S, Caccamo A, Kitazawa M, Tseng BP, LaFerla FM. Amyloid deposition precedes tangle formation in a triple transgenic model of Alzheimer's disease. *Neurobiol Aging.* 2003; 24:1063–1070. [PubMed: 14643377]
28. Oddo S, Caccamo A, Green KN, Liang K, Tran L, Chen Y, Leslie FM, LaFerla FM. Chronic nicotine administration exacerbates tau pathology in a transgenic model of Alzheimer's disease. *Proc Natl Acad Sci U S A.* 2005; 102:3046–3051. [PubMed: 15705720]
29. Oddo S, Caccamo A, Tran L, Lambert MP, Glabe CG, Klein WL, LaFerla FM. Temporal profile of amyloid- $\beta$  (A $\beta$ ) oligomerization in an *in vivo* model of Alzheimer disease. A link between A $\beta$  and tau pathology. *J Biol Chem.* 2006; 281:1599–1604. [PubMed: 16282321]
30. Billings LM, Oddo S, Green KN, McLaugh JL, LaFerla FM. Intraneuronal A $\beta$  causes the onset of early Alzheimer's disease-related cognitive deficits in transgenic mice. *Neuron.* 2005; 45:675–688. [PubMed: 15748844]
31. Hirata-Fukae C, Li HF, Hoe HS, Gray AJ, Minami SS, Hamada K, Niikura T, Hua F, Tsukagoshi-Nagai H, Horikoshi-Sakuraba Y, Mughal M, Rebeck GW, LaFerla FM, Mattson MP, Iwata N, Saido TC, Klein WL, Duff KE, Aisen PS, Matsuoka Y. Females exhibit more extensive amyloid, but not tau, pathology in an Alzheimer transgenic model. *Brain Res.* 2008; 1216:92–103. [PubMed: 18486110]
32. D'Hooge R, De Deyn PP. Applications of the Morris water maze in the study of learning and memory. *Brain Res Brain Res Rev.* 2001; 36:60–90. [PubMed: 11516773]
33. Deacon RM, Rawlins JN. T-maze alternation in the rodent. *Nat Protoc.* 2006; 1:7–12. [PubMed: 17406205]
34. Lalonde R. The neurobiological basis of spontaneous alternation. *Neurosci Biobehav Rev.* 2002; 26:91–104. [PubMed: 11835987]
35. Muscat R, Willner P. Suppression of sucrose drinking by chronic mild unpredictable stress: A methodological analysis. *Neurosci Biobehav Rev.* 1992; 16:507–517. [PubMed: 1480347]
36. Sakic B, Denburg JA, Denburg SD, Szechtman H. Blunted sensitivity to sucrose in autoimmune MRL-*lpr* mice: A curve-shift study. *Brain Res Bull.* 1996; 41:305–311. [PubMed: 8924042]
37. Sakic B, Szechtman H, Braciak TA, Richards CD, Gaudie J, Denburg JA. Reduced preference for sucrose in autoimmune mice: A possible role of interleukin-6. *Brain Res Bull.* 1997; 44:155–165. [PubMed: 9292205]

38. Sakic B, Szechtman H, Talangbayan H, Denburg SD, Carbotte RM, Denburg JA. Disturbed emotionality in autoimmune MRL-lpr mice. *Physiol Behav.* 1994; 56:609–617. [PubMed: 7972416]
39. Anisman H, Hayley S, Kelly O, Borowski T, Merali Z. Psychogenic, neurogenic, and systemic stressor effects on plasma corticosterone and behavior: Mouse strain-dependent outcomes. *Behav Neurosci.* 2001; 115:443–454. [PubMed: 11345969]
40. Edwards DA, Thompson ML, Burge KG. Olfactory bulb removal vs peripherally induced anosmia: Differential effects on the aggressive behavior of male mice. *Behav Biol.* 1972; 7:823–828. [PubMed: 4676291]
41. Yang M, Crawley JN. Simple behavioral assessment of mouse olfaction. *Curr Protoc Neurosci.* 2009 Chapter 8, Unit 8.24.
42. Kapadia M, Stanojcic M, Earls AM, Pulapaka S, Lee J, Sakic B. Altered olfactory function in the MRL model of CNS lupus. *Behav Brain Res.* 2012; 234:303–311. [PubMed: 22796602]
43. Sakic B, Szechtman H, Keffer M, Talangbayan H, Stead R, Denburg JA. A behavioral profile of autoimmune lupus-prone MRL mice. *Brain Behav Immun.* 1992; 6:265–285. [PubMed: 1392101]
44. Helyer BJ, Howie JB. Spontaneous auto-immune disease in NZB/BL mice. *Br J Haematol.* 1963; 9:119–131. [PubMed: 13953665]
45. Mebius RE, Kraal G. Structure and function of the spleen. *Nat Rev Immunol.* 2005; 5:606–616. [PubMed: 16056254]
46. Langeveld M, Gamadia LE, Ten B I. T-lymphocyte subset distribution in human spleen. *Eur J Clin Invest.* 2006; 36:250–256. [PubMed: 16620287]
47. Rosas-Ballina M, Olofsson PS, Ochani M, Valdes-Ferrer SI, Levine YA, Reardon C, Tusche MW, Pavlov VA, Andersson U, Chavan S, Mak TW, Tracey KJ. Acetylcholine-synthesizing T cells relay neural signals in a vagus nerve circuit. *Science.* 2011; 334:98–101. [PubMed: 21921156]
48. Tracey KJ. Understanding immunity requires more than immunology. *Nat Immunol.* 2010; 11:561–564. [PubMed: 20562838]
49. Tung JW, Heydari K, Tirouvanziam R, Sahaf B, Parks DR, Herzenberg LA, Herzenberg LA. *Modern flow cytometry: A practical approach.* Clin Lab Med. 2007; 27:453–468. v. [PubMed: 17658402]
50. Herzenberg LA, Tung J, Moore WA, Herzenberg LA, Parks DR. Interpreting flow cytometry data: A guide for the perplexed. *Nat Immunol.* 2006; 7:681–685. [PubMed: 16785881]
51. Saing T, Dick M, Nelson PT, Kim RC, Cribbs DH, Head E. Frontal cortex neuropathology in dementia pugilistica. *J Neurotrauma.* 2012; 29:1054–1070. [PubMed: 22017610]
52. Kitamoto T, Ogomori K, Tateishi J, Prusiner SB. Formic acid pretreatment enhances immunostaining of cerebral and systemic amyloids. *Lab Invest.* 1987; 57:230–236. [PubMed: 2441141]
53. Grundman M, Petersen RC, Ferris SH, Thomas RG, Aisen PS, Bennett DA, Foster NL, Jack CR Jr, Galasko DR, Doody R, Kaye J, Sano M, Mohs R, Gauthier S, Kim HT, Jin S, Schultz AN, Schafer K, Mulnard R, van Dyck CH, Mintzer J, Zamrini EY, Cahn-Weiner D, Thal LJ. Mild cognitive impairment can be distinguished from Alzheimer disease and normal aging for clinical trials. *Arch Neurol.* 2004; 61:59–66. [PubMed: 14732621]
54. Romberg C, Mattson MP, Mughal MR, Bussey TJ, Saksida LM. Impaired attention in the 3xTgAD mouse model of Alzheimer's disease: Rescue by donepezil (Aricept). *J Neurosci.* 2011; 31:3500–3507. [PubMed: 21368062]
55. Gimenez-Llort L, Blazquez G, Canete T, Johansson B, Oddo S, Tobena A, LaFerla FM, Fernandez-Teruel A. Modeling behavioral and neuronal symptoms of Alzheimer's disease in mice: A role for intraneuronal amyloid. *Neurosci Biobehav Rev.* 2007; 31:125–147. [PubMed: 17055579]
56. Gimenez-Llort L, Rivera-Hernandez G, Marin-Argany M, Sanchez-Quesada JL, Villegas S. Early intervention in the 3xTg-AD mice with an amyloid beta-antibody fragment ameliorates first hallmarks of Alzheimer disease. *MAbs.* 2013; 5:665–677. [PubMed: 23884018]
57. Espana J, Gimenez-Llort L, Valero J, Minano A, Rabano A, Rodriguez-Alvarez J, LaFerla FM, Saura CA. Intraneuronal beta-amyloid accumulation in the amygdala enhances fear and anxiety in Alzheimer's disease transgenic mice. *Biol Psychiatry.* 2010; 67:513–521. [PubMed: 19664757]

58. Pietropaolo S, Sun Y, Li R, Brana C, Feldon J, Yee BK. Limited impact of social isolation on Alzheimer-like symptoms in a triple transgenic mouse model. *Behav Neurosci*. 2009; 123:181–195. [PubMed: 19170443]
59. Sterniczuk R, Antle MC, LaFerla FM, Dyck RH. Characterization of the 3xTg-AD mouse model of Alzheimer's disease: Part 2. Behavioral and cognitive changes. *Brain Res*. 2010; 1348:149–155. [PubMed: 20558146]
60. Cassano T, Romano A, Macheda T, Colangeli R, Cimmino CS, Petrella A, LaFerla FM, Cuomo V, Gaetani S. Olfactory memory is impaired in a triple transgenic model of Alzheimer disease. *Behav Brain Res*. 2011; 224:408–412. [PubMed: 21741995]
61. Wilson RS, Schneider JA, Arnold SE, Tang Y, Boyle PA, Bennett DA. Olfactory identification and incidence of mild cognitive impairment in older age. *Arch Gen Psychiatry*. 2007; 64:802–808. [PubMed: 17606814]
62. Lojkowska W, Sawicka B, Gugala M, Sienkiewicz-Jarosz H, Bochynska A, Scinska A, Korkosz A, Lojek E, Ryglewicz D. Follow-up study of olfactory deficits, cognitive functions, and volume loss of medial temporal lobe structures in patients with mild cognitive impairment. *Curr Alzheimer Res*. 2011; 8:689–698. [PubMed: 21592056]
63. Devanand DP, Michaels-Marston KS, Liu X, Pelton GH, Padilla M, Marder K, Bell K, Stern Y, Mayeux R. Olfactory deficits in patients with mild cognitive impairment predict Alzheimer's disease at follow-up. *Am J Psychiatry*. 2000; 157:1399–1405. [PubMed: 10964854]
64. Gimenez-Llort L, Mate I, Manassra R, Vida C, De la FM. Peripheral immune system and neuroimmune communication impairment in a mouse model of Alzheimer's disease. *Ann N Y Acad Sci*. 2012; 1262:74–84. [PubMed: 22823438]
65. Mastrangelo MA, Bowers WJ. Detailed immunohistochemical characterization of temporal and spatial progression of Alzheimer's disease-related pathologies in male triple-transgenic mice. *BMC Neurosci*. 2008; 9:81. [PubMed: 18700006]
66. Garcia-Mesa Y, Gimenez-Llort L, Lopez LC, Venegas C, Cristofol R, Escames G, Cuna-Castroviejo D, Sanfeliu C. Melatonin plus physical exercise are highly neuroprotective in the 3xTg-AD mouse. *Neurobiol Aging*. 2012; 33:1124–1129. [PubMed: 22177720]
67. Garcia-Mesa Y, Lopez-Ramos JC, Gimenez-Llort L, Revilla S, Guerra R, Gruart A, LaFerla FM, Cristofol R, gado-Garcia JM, Sanfeliu C. Physical exercise protects against Alzheimer's disease in 3xTg-AD mice. *J Alzheimers Dis*. 2011; 24:421–454. [PubMed: 21297257]
68. Hu YS, Xu P, Pigino G, Brady ST, Larson J, Lazarov O. Complex environment experience rescues impaired neurogenesis, enhances synaptic plasticity, and attenuates neuropathology in familial Alzheimer's disease-linked APP<sup>sw</sup>/PS1<sup>DeltaE9</sup> mice. *FASEB J*. 2010; 24:1667–1681. [PubMed: 20086049]
69. Berardi N, Braschi C, Capsoni S, Cattaneo A, Maffei L. Environmental enrichment delays the onset of memory deficits and reduces neuropathological hallmarks in a mouse model of Alzheimer-like neurodegeneration. *J Alzheimers Dis*. 2007; 11:359–370. [PubMed: 17851186]
70. Cracchiolo JR, Mori T, Nazian SJ, Tan J, Potter H, Arendash GW. Enhanced cognitive activity—over and above social or physical activity—is required to protect Alzheimer's mice against cognitive impairment, reduce Abeta deposition, and increase synaptic immunoreactivity. *Neurobiol Learn Mem*. 2007; 88:277–294. [PubMed: 17714960]
71. Jonsson T, Stefansson H, Steinberg S, Jonsdottir I, Jonsson PV, Snaedal J, Bjornsson S, Huttenlocher J, Levey AI, Lah JJ, Rujescu D, Hampel H, Giegling I, Andreassen OA, Engedal K, Ulstein I, Djurovic S, Ibrahim-Verbaas C, Hofman A, Ikram MA, van Duijn CM, Thorsteinsdottir U, Kong A, Stefansson K. Variant of TREM2 associated with the risk of Alzheimer's disease. *N Engl J Med*. 2013; 368:107–116. [PubMed: 23150908]
72. Sardi F, Fassina L, Venturini L, Inguscio M, Guerriero F, Rolfo E, Ricevuti G. Alzheimer's disease, autoimmunity and inflammation. The good, the bad and the ugly. *Autoimmun Rev*. 2011; 11:149–153. [PubMed: 21996556]
73. Ghosh S, Wu MD, Shaftel SS, Kyrkanides S, LaFerla FM, Olschowka JA, O'Banion MK. Sustained interleukin-1beta overexpression exacerbates tau pathology despite reduced amyloid burden in an Alzheimer's mouse model. *J Neurosci*. 2013; 33:5053–5064. [PubMed: 23486975]

74. Sy M, Kitazawa M, Medeiros R, Whitman L, Cheng D, Lane TE, LaFerla FM. Inflammation induced by infection potentiates tau pathological features in transgenic mice. *Am J Pathol.* 2011; 178:2811–2822. [PubMed: 21531375]
75. Krstic D, Madhusudan A, Doehner J, Vogel P, Notter T, Imhof C, Manalastas A, Hilfiker M, Pfister S, Schwerdel C, Riether C, Meyer U, Knuesel I. Systemic immune challenges trigger and drive Alzheimer-like neuropathology in mice. *J Neuroinflammation.* 2012; 9:151. [PubMed: 22747753]
76. Cowley SC, Meierovics AI, Frelinger JA, Iwakura Y, Elkins KL. Lung CD4-CD8-double-negative T cells are prominent producers of IL-17A and IFN-gamma during primary respiratory murine infection with *Francisella tularensis* live vaccine strain. *J Immunol.* 2010; 184:5791–5801. [PubMed: 20393138]
77. Villani FN, Rocha MO, Nunes MC, Antonelli LR, Magalhaes LM, dos Santos JS, Gollob KJ, Dutra WO. Trypanosoma cruzi-induced activation of functionally distinct alphabeta and gammadelta CD4- CD8- T cells in individuals with polar forms of Chagas' disease. *Infect Immun.* 2010; 78:4421–4430. [PubMed: 20696836]
78. D'Acquisto F, Crompton T. CD3+CD4-CD8- (double negative) T cells: Saviours or villains of the immune response? *Biochem Pharmacol.* 2011; 82:333–340. [PubMed: 21640713]
79. Reinhardt C, Melms A. Normalization of elevated CD4-/CD8- (double-negative) T cells after thymectomy parallels clinical remission in myasthenia gravis associated with thymic hyperplasia but not thymoma. *Ann Neurol.* 2000; 48:603–608. [PubMed: 11026443]
80. Crispin JC, Oukka M, Bayliss G, Cohen RA, Van Beek CA, Stillman IE, Kyttaris VC, Juang YT, Tsokos GC. Expanded double negative T cells in patients with systemic lupus erythematosus produce IL-17 and infiltrate the kidneys. *J Immunol.* 2008; 181:8761–8766. [PubMed: 19050297]
81. Merino R, Fossati L, Iwamoto M, Takahashi S, Lemoine R, Ibnou-Zekri N, Pugliatti L, Merino J, Izui S. Effect of long-term anti-CD4 or anti-CD8 treatment on the development of lpr CD4- CD8- double negative T cells and of the autoimmune syndrome in MRL-lpr/lpr mice. *J Autoimmun.* 1995; 8:33–45. [PubMed: 7734035]
82. Mruthinti S, Buccafusco JJ, Hill WD, Waller JL, Jackson TW, Zamrini EY, Schade RF. Autoimmunity in Alzheimer's disease: Increased levels of circulating IgGs binding Abeta and RAGE peptides. *Neurobiol Aging.* 2004; 25:1023–1032. [PubMed: 15212827]
83. Dorothee G, Bottlaender M, Moukari E, de Souza LC, Maroy R, Corlier F, Colliot O, Chupin M, Lamari F, Lehericy S, Dubois B, Sarazin M, Aucouturier P. Distinct patterns of anti-amyloid-beta antibodies in typical and atypical Alzheimer disease. *Arch Neurol.* 2012; 69:1181–1185. [PubMed: 22710357]
84. Nath A, Hall E, Tuzova M, Dobbs M, Jons M, Anderson C, Woodward J, Guo Z, Fu W, Kryscio R, Wekstein D, Smith C, Markesbery WR, Mattson MP. Autoantibodies to amyloid beta-peptide (Abeta) are increased in Alzheimer's disease patients and Abeta antibodies can enhance Abeta neurotoxicity: Implications for disease pathogenesis and vaccine development. *Neuromolecular Med.* 2003; 3:29–39. [PubMed: 12665674]
85. D'Andrea MR. Evidence linking neuronal cell death to autoimmunity in Alzheimer's disease. *Brain Res.* 2003; 982:19–30. [PubMed: 12915236]
86. Gerendai I, Halasz B. Neuroendocrine asymmetry. *Front Neuroendocrinol.* 1997; 18:354–381. [PubMed: 9237081]
87. Hebda-Bauer EK, Simmons TA, Sugg A, Ural E, Stewart JA, Beals JL, Wei Q, Watson SJ, Akil H. 3xTg-AD mice exhibit an activated central stress axis during early-stage pathology. *J Alzheimers Dis.* 2013; 33:407–422. [PubMed: 22976078]
88. Michaud M, Balardy L, Moulis G, Gaudin C, Peyrot C, Vellas B, Cesari M, Nourhashemi F. Proinflammatory cytokines, aging, and age-related diseases. *J Am Med Dir Assoc.* 2013 pii: S1525-8610(13)00280-6. doi: 10.1016/j.jamda.2013.05.009.
89. Gimenez-Llort L, Arranz L, Mate I, De la FM. Gender-specific neuroimmunoendocrine aging in a tripletransgenic 3xTg-AD mouse model for Alzheimer's disease and its relation with longevity. *Neuroimmunomodulation.* 2008; 15:331–343. [PubMed: 19047809]
90. Prelog M. Aging of the immune system: A risk factor for autoimmunity? *Autoimmun Rev.* 2006; 5:136–139. [PubMed: 16431345]

91. Maftai M, Thurm F, Schnack C, Tumani H, Otto M, Elbert T, Kolassa IT, Przybylski M, Manea M, von Arnim CA. Increased levels of antigenbound beta-amyloid autoantibodies in serum and cerebrospinal fluid of Alzheimer's disease patients. *PLoS ONE*. 2013; 8:e68996. [PubMed: 23874844]
92. Monsonego A, Nemirovsky A, Harpaz I. CD4 T cells in immunity and immunotherapy of Alzheimer's disease. *Immunology*. 2013; 139:438–446. [PubMed: 23534386]
93. Mengel D, Roskam S, Neff F, Balakrishnan K, Deuster O, Gold M, Oertel WH, Bacher M, Bach JP, Dodel R. Naturally occurring autoantibodies interfere with beta-amyloid metabolism and improve cognition in a transgenic mouse model of Alzheimer's disease 24h after single treatment. *Transl Psychiatry*. 2013; 3:e236. [PubMed: 23462987]
94. Holmes C, Cunningham C, Zotova E, Culliford D, Perry VH. Proinflammatory cytokines, sickness behavior, and Alzheimer disease. *Neurology*. 2011; 77:212–218. [PubMed: 21753171]
95. Forlenza OV, Diniz BS, Talib LL, Mendonca VA, Ojopi EB, Gattaz WF, Teixeira AL. Increased serum IL-1beta level in Alzheimer's disease and mild cognitive impairment. *Dement Geriatr Cogn Disord*. 2009; 28:507–512. [PubMed: 19996595]
96. Banks WA, Erickson MA. The blood-brain barrier and immune function and dysfunction. *Neurobiol Dis*. 2010; 37:26–32. [PubMed: 19664708]
97. Xiong H, Callaghan D, Jones A, Bai J, Rasquinha I, Smith C, Pei K, Walker D, Lue LF, Stanimirovic D, Zhang W. ABCG2 is upregulated in Alzheimer's brain with cerebral amyloid angiopathy and may act as a gatekeeper at the blood-brain barrier for Abeta(1-40) peptides. *J Neurosci*. 2009; 29:5463–5475. [PubMed: 19403814]
98. Douglas SA, Sreenivasan D, Carman FH, Bunn SJ. Cytokine interactions with adrenal medullary chromaffin cells. *Cell Mol Neurobiol*. 2010; 30:1467–1475. [PubMed: 21088883]
99. Renner U, De Santana EC, Gerez J, Frohlich B, Haedo M, Pereda MP, Onofri C, Stalla GK, Arzt E. Intrapituitary expression and regulation of the gp130 cytokine interleukin-6 and its implication in pituitary physiology and pathophysiology. *Ann N Y Acad Sci*. 2009; 1153:89–97. [PubMed: 19236332]
100. Landfield PW, Blalock EM, Chen KC, Porter NM. A new glucocorticoid hypothesis of brain aging: Implications for Alzheimer's disease. *Curr Alzheimer Res*. 2007; 4:205–212. [PubMed: 17430248]
101. Silverman MN, Sternberg EM. Glucocorticoid regulation of inflammation and its functional correlates: From HPA axis to glucocorticoid receptor dysfunction. *Ann N Y Acad Sci*. 2012; 1261:55–63. [PubMed: 22823394]
102. Esteras N, Alquezar C, Bartolome F, Antequera D, Barrios L, Carro E, Cerdan S, Martin-Requero A. Systematic evaluation of magnetic resonance imaging and spectroscopy techniques for imaging a transgenic model of Alzheimer's disease (AbetaPP/PS1). *J Alzheimers Dis*. 2012; 30:337–353. [PubMed: 22406445]
103. Masdeu JC, Kreisl WC, Berman KF. The neurobiology of Alzheimer disease defined by neuroimaging. *Curr Opin Neurol*. 2012; 25:410–420. [PubMed: 22766722]
104. Schwab C, Klegeris A, McGeer PL. Inflammation in transgenic mouse models of neurodegenerative disorders. *Biochim Biophys Acta*. 2010; 1802:889–902. [PubMed: 19883753]
105. Gahtan E, Overmier JB. Inflammatory pathogenesis in Alzheimer's disease: Biological mechanisms and cognitive sequelae. *Neurosci Biobehav Rev*. 1999; 23:615–633. [PubMed: 10392655]
106. Bouras C, Riederer BM, Kovari E, Hof PR, Giannakopoulos P. Humoral immunity in brain aging and Alzheimer's disease. *Brain Res Brain Res Rev*. 2005; 48:477–487. [PubMed: 15914253]
107. Cserr, HF.; Knopf, PM. Cervical lymphatics, the blood-brain barrier, and immunoreactivity of the brain.. In: Keane, RW.; Hickey, WF., editors. *Immunology of the Nervous System*. Oxford University Press; New York: 1997. p. 134-152.
108. Rosenmann H, Grigoriadis N, Karussis D, Boimel M, Touloumi O, Ovadia H, Abramsky O. Tauopathy-like abnormalities and neurologic deficits in mice immunized with neuronal tau protein. *Arch Neurol*. 2006; 63:1459–1467. [PubMed: 17030663]
109. Rosenmann H, Meiner Z, Geylis V, Abramsky O, Steinitz M. Detection of circulating antibodies against tau protein in its unphosphorylated and in its neurofibrillary tangles-related

phosphorylated state in Alzheimer's disease and healthy subjects. *Neurosci Lett.* 2006; 410:90–93. [PubMed: 17095156]

110. Anderson JM, Hampton DW, Patani R, Pryce G, Crowther RA, Reynolds R, Franklin RJ, Giovannoni G, Compston DA, Baker D, Spillantini MG, Chandran S. Abnormally phosphorylated tau is associated with neuronal and axonal loss in experimental autoimmune encephalomyelitis and multiple sclerosis. *Brain.* 2008; 131:1736–1748. [PubMed: 18567922]

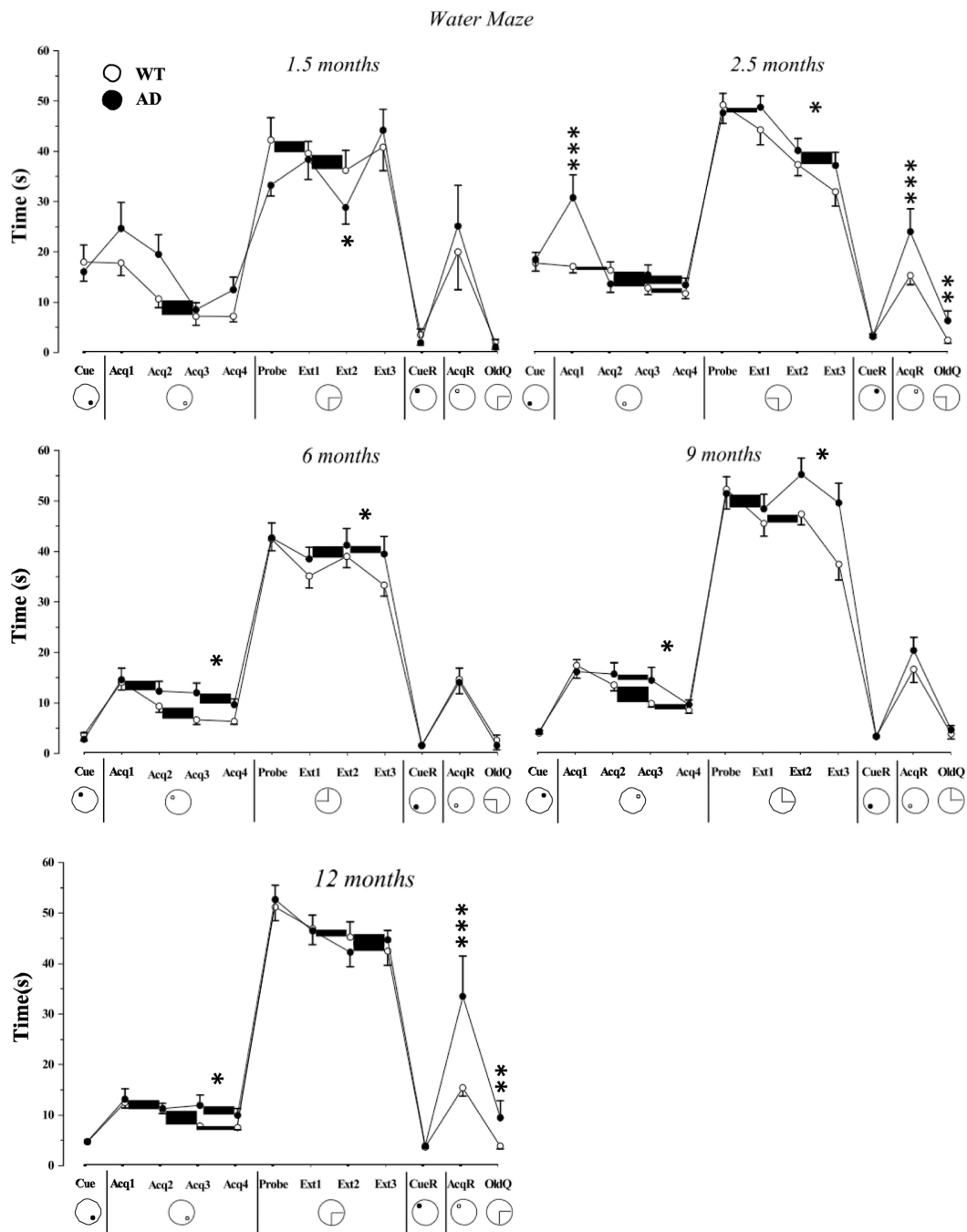


**Fig. 1.** Performance in the water maze. All groups showed comparable performance in cued trials, suggesting AD mice have no deficits in visual acuity and motor capacity. However, 2.5-month old AD mice displayed longer escape latencies, higher swimming speed, and increased thigmotaxis when initially exposed to a pool with a hidden platform (trend seen at 1.5 months). Expectedly, the AD group generally showed a slower rate of acquisition response. This was not due to different learning strategy because their performance in the probe trial was comparable to the control group. However, AD mice showed slower

extinction rate at several ages. When the task was made more difficult by placing the submerged platform in the opposite quadrant, 2.5-month and 12-month-old AD demonstrated an increased latency to escape, largely attributable to their perseverative response in the previous goal quadrant. Taken together, the above results suggest age-related enhancement in emotional reactivity, slower response acquisition rate, impaired extinction and cognitive inflexibility in AD mice. *Note:* Time denotes latency to find the platform in cued (Cue) and acquisition (Acq) trials, but reflects time spent in the target quadrant (Q) in probe, extinction (Ext) and “reversal” (R) trials. The position of the platform is schematically shown under the X-axis.

Author Manuscript

Author Manuscript

Author Manuscript

Author Manuscript



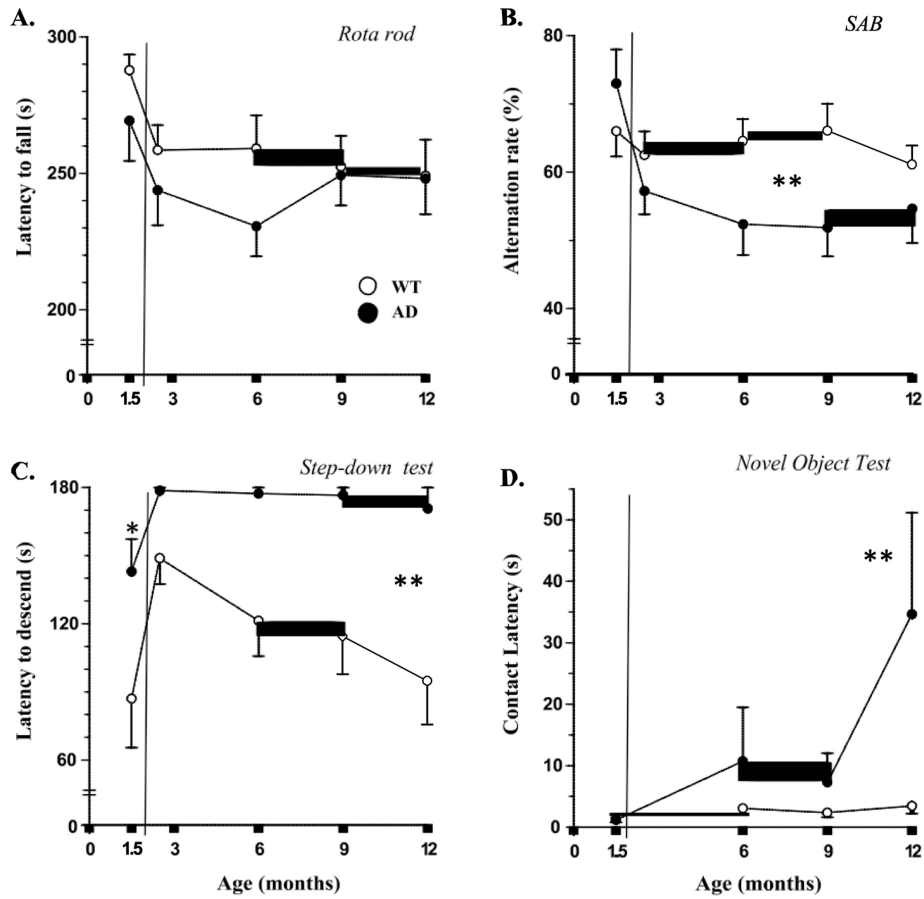


**Fig. 2.** Performance in the behavioral battery. A) Comparable fall latencies in Rota-Rod trials suggest intact sensorimotor coordination in both cohorts of animals. B) On the other hand, age-dependent reduction in the alternation rate of AD mice point to an early onset of spatial memory deficits. C) These changes are preceded by sustained anxiety-like response, as evidenced by prolonged step-down latency from an elevated platform. D) Similarly, AD mice display increased latency to approach a novel object at 12 months of age. Collectively, the above results suggest enhanced emotional reactivity precedes the development of spatial acquisition and learning/memory dysfunction in the 3xTg-AD model.

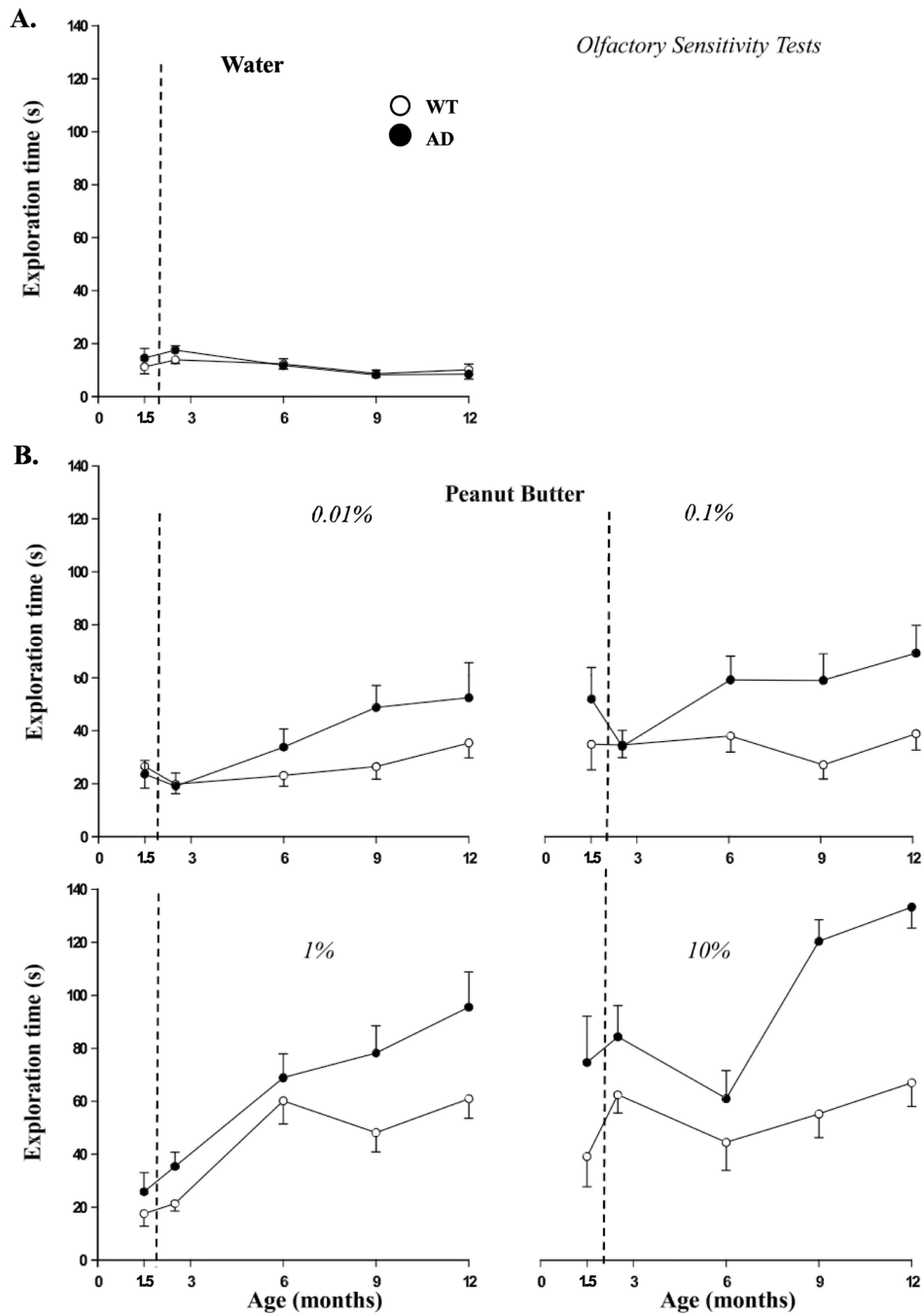


**Fig. 3.** Altered olfactory function. A) Comparable investigation of a wet filter paper across all ages in WT and AD mice. B–E) Increased response to different concentrations of peanut butter in older mice AD mice suggests the development of disease-dependent alterations in olfactory function.

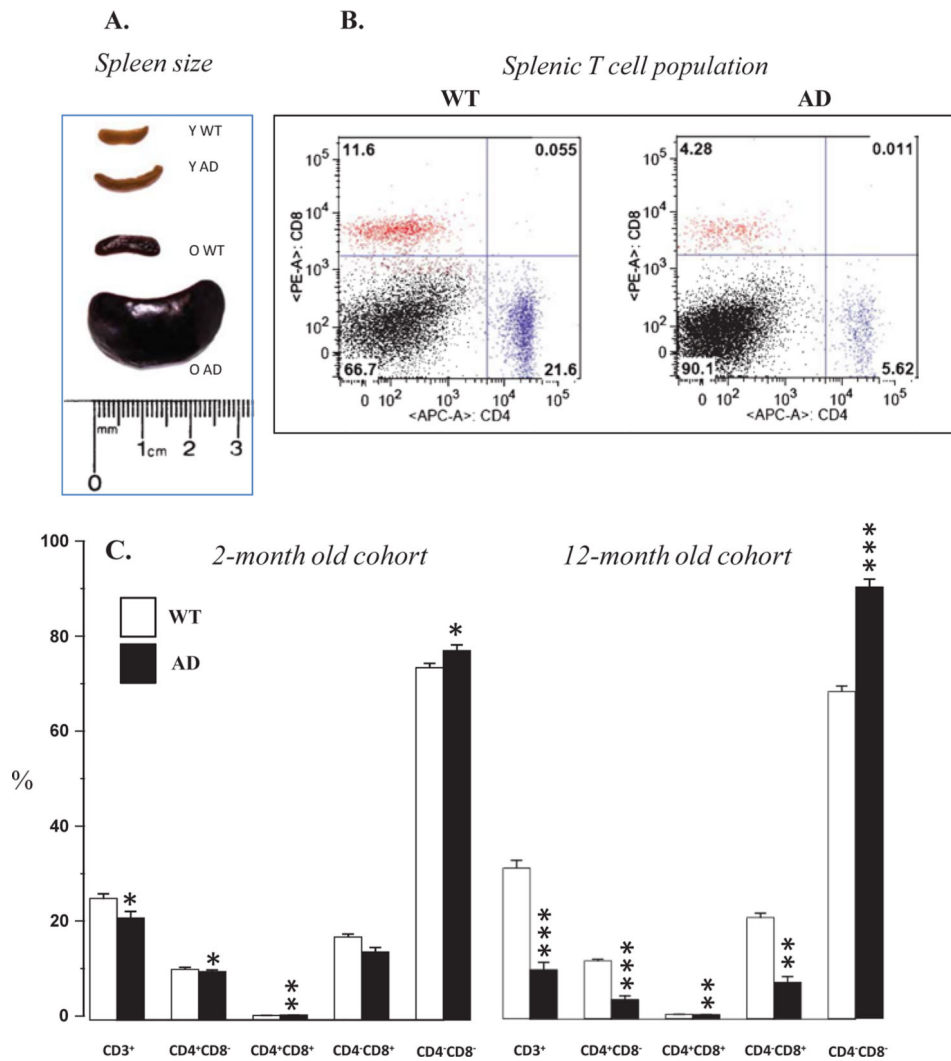
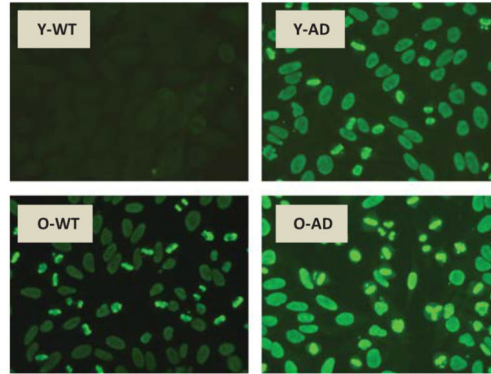
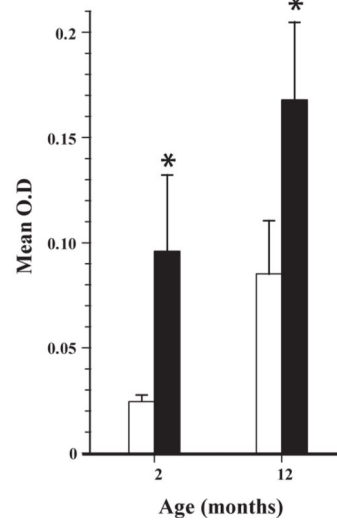


**Fig. 4.** Alterations in spleen morphology and function. A) Representative photos illustrating severity of splenomegaly in AD mice at 2 and 12 months of age. B) Representative FACS analysis of differentiating T splenocytes from aged AD and WT mice. Dot plots are representative of triplicate experiments. C) Quantitative assessment of T splenocytes points to an early, but progressive shift from CD<sup>+</sup> clones to CD double negative subpopulations, suggestive of an autoimmune-like disease in AD mice.

**A. Anti-nuclear Antibodies**



**B. Anti-dsDNA Antibodies**



**C. Hematocrit**

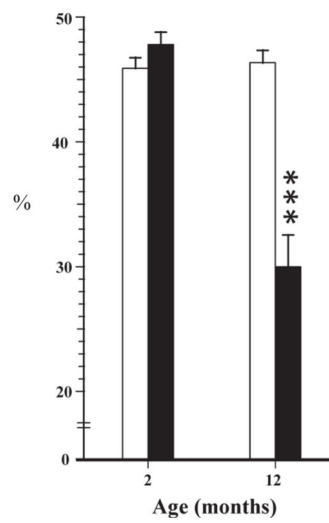


**Fig. 5.** Serological changes. A) Representative images revealing increased ANA positivity associated with aging and AD-like disease. B) Serum levels of anti-dsDNA increase with age in both groups, but AD mice display an early and sustained elevation. C) Significantly lower hematocrit in aged AD mice suggests autoimmune hemolytic anemia that develops with more severe immunological manifestations. Y, young; O, old.

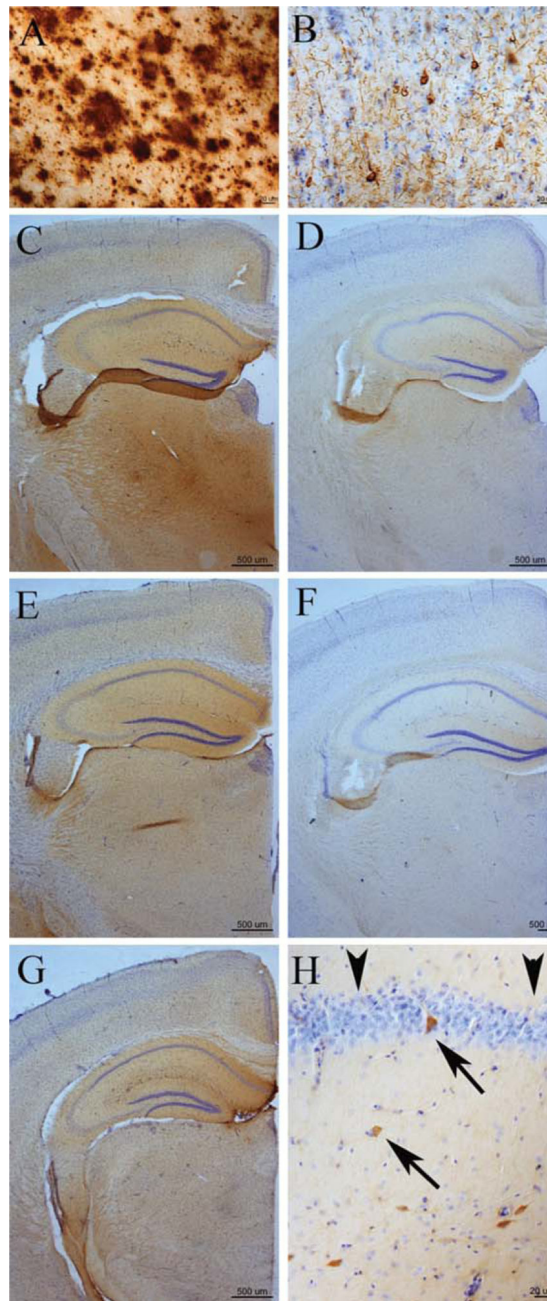


**Fig. 6.** AD-like neuropathology in 3xTg-AD and WT mice. A, B) A $\beta$  (left) and neurofibrillary tangles (right) detected in the frontal cortex of an AD case that served as a positive control. However, 6E10 positive deposits were observed neither in the 12 month old 3xTg-AD mice, (C) nor in the 12 month-old WT controls (E). AT8 immunolabeling was similar when comparing 12 month 3xTg-AD mice (D), 12 month old WT mice (F) and young 2 month-old 3xTg-AD mice (G). A higher magnification of AT8 immunolabeling in a 12-month 3xTg-AD mouse (H), showing scattered neurons positive for phosphorylated tau (arrows) in the hippocampus (arrowheads indicate area CA1). Bars in A, B and H are 20  $\mu$ m and in C–G are 500  $\mu$ m.

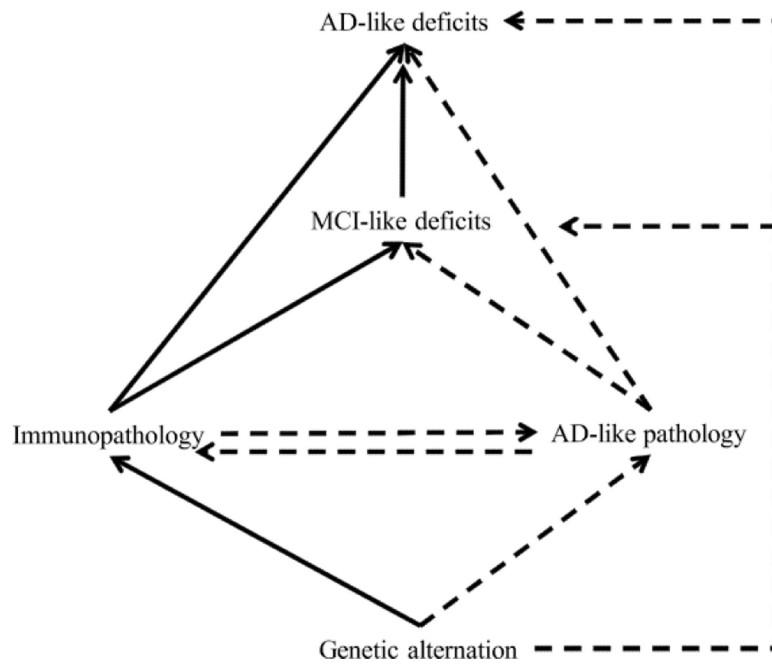


**Fig. 7.** Observed pathogenic circuitry. Although reported by other researchers in the past, we did not observe the link between altered genotype and AD-like pathology with the present sample size. One may hypothesize that genetic alterations per se contribute to behavioral deficits in the 3xTg-AD model. However, our results suggest a relationship between genetics, activation of the immune system, and altered behavior. It remains unknown if immunological phenomena contribute to neuropathological events at a later stage of AD-like disease or alternatively, early intraneuronal damage triggers a peripheral immune response. Note: Solid lines represent observed relationships, while dotted lines represent proposed relationships.

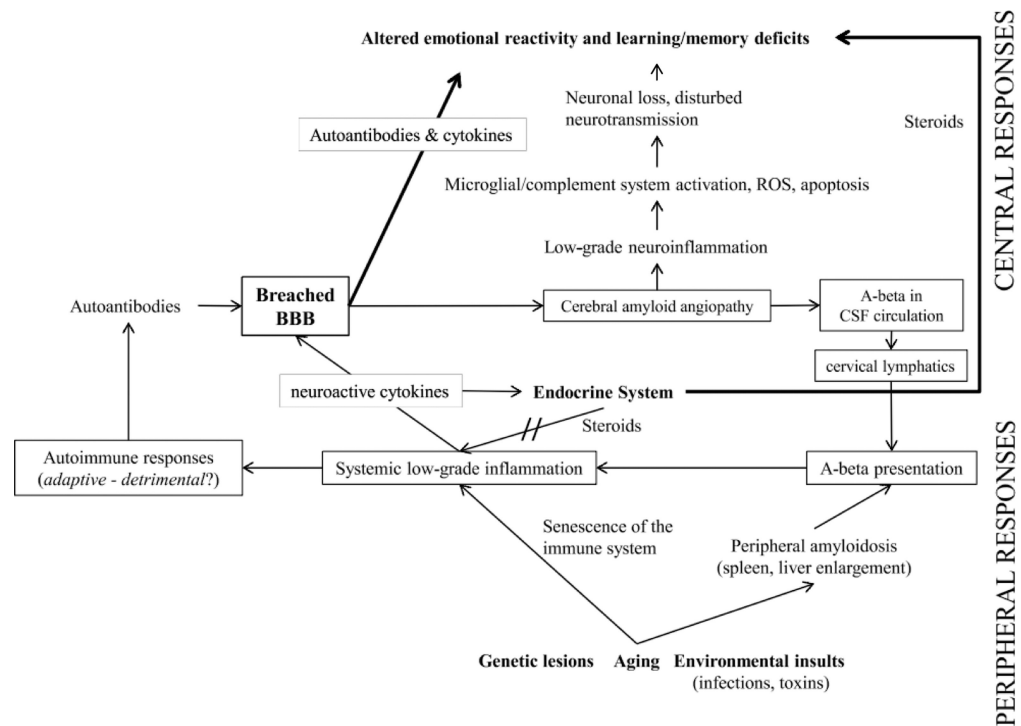


**Fig. 8.**

Proposed mechanisms in AD-like disease. Aging, genetic mutations, and environmental insults may synergistically underlie pathogenesis of AD and AD-like phenotypes. The aging process is known to be accompanied by thymic atrophy and immunosenescence [88, 89], or aberrant T cell reactivity to external and self-antigens [90]. In the case of 3xTg-AD mice, the transfer of human genes may result in excessive deposition of AB in peripheral tissues (amyloidosis), such as the spleen and liver. Chronic presentation of A $\beta$  to over-reactive T cells may result in low-grade inflammation and autoimmune responses [91], likely aimed to clear the abundant protein [56, 92, 93]. The accompanying increase in serum levels of pro-inflammatory cytokines [94, 95] may compromise the integrity of the blood-brain barrier [96], accounting for cerebral amyloid angiopathy in AD patients and the 3xTg-AD model [97]. At the same time, circulating cytokines can also activate receptors in the pituitary and adrenal glands [98, 99], thus inducing sustained production of steroids [100] to regulate inflammation [101]. However, the opening of the blood-brain barrier to large immune molecules and sustained binding of steroid hormones to cortical and limbic areas may alter emotional reactivity and induce MCI-like deficits at a prodromal stage of disease development. Severe cognitive dysfunction at the later stage of AD-like disease may be a consequence of chronic autoantibody reactivity and steroid-induced excitotoxicity, resulting in regional brain atrophy [102,103]. Subsequent CNS inflammatory responses [104], as evidenced by activation of microglia, complement system and production of reactive oxygen species [105] may further add to this insult. Tau-pathology may represent “collateral damage” induced by autoantibodies binding to microtubules, leading to their disintegration and neurofibrillary tangle formation [106]. However, cerebrospinal fluid circulation of AD-related proteins and their presentation in cervical lymph nodes [107] may

lead to maintenance and amplification of autoimmune/inflammatory response, thus further exacerbating brain damage and behavioral dysfunction [108–110].

Author Manuscript

Author Manuscript

Author Manuscript

Author Manuscript



**Table 1**

Body and organ weights at sacrifice. In both cohorts, AD mice were lighter, had lower brain mass, and displayed increased spleen weight in comparison to the WT group. These changes were accompanied by hepatomegaly and hypertrophy of the right adrenal gland at an older age. Taken together, age-dependent increases in peripheral organ weights suggests an ongoing systemic process in 3xTg-AD mice. (*Note:* Significant group differences are shown in bold)

Strain ( <i>sample size</i> )	Age ( <i>months</i> )	Body weight (g)	Brain (mg)	Spleen (mg)	Liver (g)	Right adrenal gland (mg)	Left adrenal gland (mg)	Right kidney (g)	Left kidney (g)
WT ( <i>n</i> = 10)	2	26.67 ± 0.61	491 ± 6	70 ± 4	1.11 ± 0.02	1.12 ± 0.08	1.53 ± 0.1	0.21 ± 0.01	0.2 ± 0.01
AD ( <i>n</i> = 10)		<b>23.23 ± 0.46</b>	<b>439 ± 5</b>	<b>90 ± 7</b>	0.97 ± 0.24	1.27 ± 0.12	1.45 ± 0.07	0.19 ± 0.01	0.19 ± 0.01
WT ( <i>n</i> = 20)	12	43.61 ± 1.01	522 ± 5	123 ± 9	1.97 ± 0.09	1.35 ± 0.09	1.58 ± 0.11	0.32 ± 0.01	0.31 ± 0.01
AD ( <i>n</i> = 17)		<b>38.05 ± 1.14</b>	<b>475 ± 10</b>	<b>2354 ± 404</b>	<b>3.04 ± 0.33</b>	<b>1.89 ± 0.15</b>	1.74 ± 0.16	0.32 ± 0.01	0.31 ± 0.01